



Published in final edited form as:

*Microsc Res Tech.* 2001 December 1; 55(5): 307–329.

## Recent Advances in Insect Olfaction, Specifically Regarding the Morphology and Sensory Physiology of Antennal Sensilla of the Female Sphinx Moth *Manduca sexta*

VONNIE D.C. SHIELDS<sup>1,\*</sup> and JOHN G. HILDEBRAND<sup>2</sup>

<sup>1</sup>Biological Sciences Department, Towson University, Towson, Maryland 21252

<sup>2</sup>Arizona Research Laboratories Division of Neurobiology, Tucson, Arizona 85721

### Abstract

The antennal flagellum of female *Manduca sexta* bears eight sensillum types: two trichoid, two basiconic, one auriculate, two coeloconic, and one styliform complex sensilla. The first type of trichoid sensillum averages 34  $\mu\text{m}$  in length and is innervated by two sensory cells. The second type averages 26  $\mu\text{m}$  in length and is innervated by either one or three sensory cells. The first type of basiconic sensillum averages 22  $\mu\text{m}$  in length, while the second type averages 15  $\mu\text{m}$  in length. Both types are innervated by three bipolar sensory cells. The auriculate sensillum averages 4  $\mu\text{m}$  in length and is innervated by two bipolar sensory cells. The coeloconic type-A and type-B both average 2  $\mu\text{m}$  in length. The former type is innervated by five bipolar sensory cells, while the latter type, by three bipolar sensory cells. The styliform complex sensillum occurs singly on each annulus and averages 38–40  $\mu\text{m}$  in length. It is formed by several contiguous sensilla. Each unit is innervated by three bipolar sensory cells. A total of 2,216 sensilla were found on a single annulus (annulus 21) of the flagellum. Electrophysiological responses from type-A trichoid sensilla to a large panel of volatile odorants revealed three different subsets of olfactory receptor cells (ORCs). Two subsets responded strongly to only a narrow range of odorants, while the third responded strongly to a broad range of odorants. Anterograde labeling of ORCs from type-A trichoid sensilla revealed that their axons projected mainly to two large female glomeruli of the antennal lobe.

### Keywords

antennal lobe; chemosensory; electron microscopy; electrophysiology; receptor cell

### INTRODUCTION

Insects, such as moths, possess paired antennae that are endowed with a multitude of minute sensory organs or antennal sensilla. These sensilla are the crucial interface between the outer world and the nervous system of the insect. Olfactory receptor cells (ORCs) housed in these sensilla are designed to detect environmental status and change and to transmit the information regarding the nature of this change to the central nervous system. Sensilla distinguish stimuli of several modalities (olfaction, taste, mechanoreception, thermoreception, and hygroreception). The vast majority of antennal sensilla of moths are specialized to identify chemosensory information, especially olfactory stimuli. Odor molecules first reach the surface of an olfactory sensillum, which is perforated by numerous small pores, and then find their

\*Correspondence to: Dr. Vonnice D.C. Shields, Biological Sciences Department, Towson University, Towson, MD 21252. E-mail: vshields@towson.edu

way to the underlying sensory neurons. Here, the chemical signal is converted into an electrical one that is sent to the brain of the insect.

The behavior of moths is controlled to a large extent by olfactory stimuli. Moths depend principally on olfactory cues to locate mates, food sources, and oviposition sites. Until now, research on moth olfaction concentrated mainly on the male's responses to the sex pheromone emitted by a conspecific female. Very little is known about the olfactory system of female moths. Female moths find host plants through odor-mediated behavior. They detect volatile chemicals that indicate host plant suitability and also the presence of potential competitors or co-habitants (Hansson, 1995). More-over, volatiles emitted by flowers help both foraging males and females to locate nectar sources. Our research has focused on understanding how the female sphinx moth *Manduca sexta* detects host-associated volatiles, how olfactory information about them is conveyed to the brain by the sensory cells housed within antennal olfactory sensilla, and how this information is used in orienting to and selecting oviposition sites.

Female *M. sexta* oviposit preferentially on various plants in the family Solanaceae (Yamamoto et al., 1969). These include certain night-blooming plants (e.g., jimson weed, *Datura wrightii*) (Raguso et al., 1996; Raguso and Light, 1998), tomato (*Lycopersicon* spp.), tobacco (*Nicotiana* spp.; Yamamoto et al., 1969), as well as to devil's claw (*Proboscidea* spp.), a hostplant in the family Martyniaceae (Mechaber and Hildebrand, 2000). Like other hawkmoths, female *M. sexta* are attracted to these plants using olfactory cues present in odor emitted by those plants (Yamamoto et al., 1969). Thus, hostplant odor plays an important role for the selection of oviposition sites for *M. sexta*, as well as for other species of moths and herbivorous insects in general (Hansson, 1995; Metcalf, 1987; Ramaswamy, 1988; Renwick, 1989).

The sphinx moth *M. sexta* has become well established as a valuable experimental model for studies of the development, functional organization, and physiology of the olfactory system (e.g., see reviews by Boeckh and Tolbert, 1993; Hildebrand, 1996; Hildebrand et al., 1997). Building on earlier studies that focused mainly on the male-specific subsystem dedicated to detection and processing of sex-pheromonal information, we have carried out a detailed investigation of the antennal olfactory system of female *M. sexta*. Here, we describe the fine structure of sensilla on the antennal flagellum of female *M. sexta* and perform a functional analysis of the most numerous sensillum type, the type-A trichoid sensillum, in addition to a neuronal tracing study of ORC axonal projections to the olfactory bulb in the brain of the moth. This work on female *M. sexta*, together with those from earlier studies of male *M. sexta* (Keil, 1989; Lee and Strausfeld, 1990; Sanes and Hildebrand, 1976), provide a comprehensive morphological basis for future physiological and developmental investigations of the olfactory system in this species.

## ANTENNAL STRUCTURE

The antennae of female and male *M. sexta* comprise three segments, two small basal segments (scape and pedicel) and a long distal flagellum (Sanes and Hildebrand, 1976). The antennal flagellum in both sexes is about 2 cm long and is divided into about 80 or more subsegments (annuli or flagellomeres) (Sanes and Hildebrand, 1976). Each female antenna has approximately  $3.0 \times 10^5$ - $3.4 \times 10^5$  ORCs (Oland and Tolbert, 1988) associated with about  $10^5$  sensilla (Keil, 1989; Lee and Strausfeld, 1990; Sanes and Hildebrand, 1976; Shields and Hildebrand, 1999a,b). Similarly, there are about  $3.3 \times 10^5$  ORCs associated with about  $10^5$  sensilla in males (Keil, 1989; Lee and Strausfeld, 1990; Oland and Tolbert, 1989; Sanes and Hildebrand, 1976). In both sexes, each annulus bears approximately 2,100-2,200 sensilla (Lee and Strausfeld, 1990; Shields and Hildebrand, 1999b) and several sensillum types are located

on the leading (frontal, anterior, or windward), ventral, and dorsal surfaces (Fig. 1A-C) (Keil, 1989; Lee and Strausfeld, 1990; Sanes and Hildebrand, 1976; Shields and Hildebrand, 1999a,b). The trailing (rear, posterior, or leeward) surface in both sexes is densely covered by scales and has been reported in males to bear only mechanosensitive and contact chemosensory sensilla (Lee and Strausfeld, 1990).

The antennal flagellum is sexually dimorphic: it is filiform in females (Fig. 1A) and more slender than in males (Fig. 1B); female annuli are oval-shaped, whereas those of males are keyhole-shaped in cross section; and the surface area of an individual female annulus is about half that of a male annulus (Fig. 1A,B; Lee and Strausfeld, 1990; Sanes and Hildebrand, 1976). The long, hairlike male-specific trichoid sensilla are arranged as a pair of phalanxes and form an arch, one pair on the distal and proximal margins of the dorsal surface and a similar arrangement of sensilla on the ventral surface of each annulus (Fig. 1B; Keil, 1989; Lee and Strausfeld, 1990; Sanes and Hildebrand, 1976), whereas in females, these arches are absent and the hairlike sensilla are much shorter (Fig. 1A; Sanes and Hildebrand, 1976). In females, the type-A trichoid sensilla, the main sensillum type present, are found in greatest abundance in a band two to three sensilla deep along the distal and proximal margins of the leading, dorsal, and ventral surfaces of each annulus (Figs. 1C). These bands merge toward the trailing surface and form a U-shaped cul-de-sac (Shields and Hildebrand, 1999b), similar but less conspicuous than the pattern of distribution of male-specific trichoid sensilla (Lee and Strausfeld, 1990; Sanes and Hildebrand, 1976). In addition to this band, the type-A trichoid sensilla are also distributed over the leading, dorsal, and ventral surfaces (Shields and Hildebrand, 1999b), a feature that is not found in males (Lee and Strausfeld, 1990).

## SENSILLUM TYPES

There are eight types of sensilla on the antennal flagellum of the female moth, *M. sexta*: two trichoid, two basiconic, one auriculate, two coeloconic, and one styliform complex. The materials and methods used for investigating these sensilla by scanning electron-(SEM), field-emission scanning electron- (FESEM), and transmission electron microscopy (TEM) were outlined previously in Shields and Hildebrand (1999a). Morphological evidence indicates that of these eight types, five appear to be olfactory, one appears to be olfactory or olfactory-thermosensory, and two appear to be thermo-hygrosensory. Lee and Strausfeld (1990) described nine sensillum types in males (two trichoid, two basiconic, two chaetic, two coeloconic, and a styliform complex). Five of these types are thought to contribute to odor detection. Below, we describe the eight sensillum types found in female *M. sexta*.

### Types-A and -B Trichoid Sensilla

There are two types of trichoid sensilla, type-A and type-B. Both types are single-walled, multiporous sensilla that have the appearance of a hair (Figs. 1C, D, 2A, 3A, C; see also Fig. 6D). The trichoid type-A sensillum is reconstructed in a longitudinal view in Figure 7A. The trichoid type-A sensillum averages 34  $\mu\text{m}$  in length, has a diameter of 4  $\mu\text{m}$  near the base of the sensillum, and tapers to 1  $\mu\text{m}$  at the tip. The wall of the shaft averages 0.25  $\mu\text{m}$  in thickness and bears circumferential, cuticular ridges, which form a helical pattern over the basal quarter of the length of the sensillum and a more circular pattern over the remaining length of the sensillum (Fig. 2B, D, E). The shaft wall is also perforated by 13 pores per  $\mu\text{m}^2$ . Each pore averages 0.02  $\mu\text{m}$  in diameter and is located in cuticular depressions (Fig. 2B, D, E). They are arranged in a single row along the midline of the ridges (Fig. 2D, E) and extend to the tip of the sensillum. Each pore opens into a small pore kettle, from which three to five pore tubules extend through the cuticular wall, inward to the underlying sensillar sinus, and into the lumen of the shaft. The type-A trichoid sensilla are innervated by two unbranched sensory cells, whose dendrites extend to the tip of the sensillum (see Fig. 7A; Table 1).

The type-B trichoid sensillum is slightly shorter than the type-A trichoid sensillum and averages 26  $\mu\text{m}$  in length. This sensillum has a diameter of 2  $\mu\text{m}$  near its base, and tapers to 0.4  $\mu\text{m}$  at the tip. The wall of the shaft averages 0.45  $\mu\text{m}$  in thickness and has diagonal ridges that form a herringbone pattern (Fig. 2D). The shaft wall is perforated by 15 pores per  $\mu\text{m}^2$ . Each pore averages 0.3  $\mu\text{m}$  in diameter and is located in a cuticular depression. The pores are arranged in a single row along the distal margin of the ridges (Fig. 2D). The pores are found up to the tip of the sensillum. Similar to type-A trichoid sensilla, each pore opens into a reduced pore kettle, from which two to four pore tubules extend inward to the underlying sensillar sinus, but do not extend into the shaft lumen. Type-B sensilla are innervated by one or three unbranched sensory cells (Fig. 2C, Table 1), whose distal dendrites extend to the tip of the sensillum (see also Shields and Hildebrand, 1999a). Both types of trichoid sensilla are associated with three sheath cells (thecogen, trichogen, tormogen) (see Fig. 7A, Table 1). A more complete description of the internal fine structure of both types-A and -B trichoid sensilla, as well as the other antennal sensillum types of female *M. sexta* can be found in Shields and Hildebrand (1999a,b).

The fine structure of the trichoid sensilla of female *M. sexta* very closely resembles that of the trichoid sensilla of female and male *Bombyx mori* (Steinbrecht, 1973, 1980; Steinbrecht and Gnatzy, 1984), males of *M. sexta* (Keil, 1989; Lee and Strausfeld, 1990), *Antheraea polyphemus* (Keil, 1984a), *Antheraea pernyi* (Keil, 1984a), *Yponomeuta vigintipunctatus*, *Adoxophyes orana*, and female *Yponomeuta cagnagellus* (Cuperus, 1985a).

The importance of the pore tubule system has long been speculated. The pore tubule system was first described by Slifer et al. (1959) in the thin-walled sensilla of a grasshopper. The tubules were thought to be fine extensions of the dendrites. Ernst (1969) later disproved this idea and demonstrated that the pore tubules were not dendritic extrusions but rather cuticular intrusions formed by the trichogen cell. Several researchers demonstrated that the pore tubules actually contact the dendritic membrane (Keil, 1982; 1984a,b; Steinbrecht and Müller, 1971). Several authors have reported that pore tubules provide a conduction pathway for molecules to diffuse to the dendritic membrane. Kaissling (1974) proposed that the pore tubules could provide a direct pathway for pheromone molecules to diffuse to the dendritic membrane. Keil (1982) later reported that the core of the pore tubules may be hydrophilic, whereas the walls might be lipophilic, allowing lipophilic molecules to use the tubule wall as a diffusion pathway. Later, two hypotheses evolved involving an olfactory binding protein. The first suggested that the odorant may be transported toward the sensory cell through the pore tubules (Kaissling, 1986; Vogt and Riddiford, 1981a,b), whereas the second suggested that the odorant may be transported towards the receptor by the binding protein (Vogt, 1987; Vogt and Riddiford, 1986).

Conventional SEM was unable to provide the requisite resolution at higher magnifications to allow the unambiguous classification of all sensillum types, especially the two populations of trichoid sensilla, types-A and -B of female *M. sexta*. FESEM provided a much greater resolution capability at higher magnifications (it functions at lower accelerating voltages) and allowed greater enhancement of surface detail to be observed. Type-A trichoid sensilla of females are distinguished from type-B sensilla, since the former: (1) are slightly longer; (2) have a wider base diameter; and (3) clearly the most distinguishable feature, have a cuticular shaft with well-defined, transverse, overlapping, wide plates that are perforated by relatively few pores in the middle of each plate. These sensilla can be further differentiated by transmission electron microscopy (TEM), since type-A sensilla: (1) have thinner cuticular shafts; (2) have more pore tubules associated with each pore that extend into the shaft lumen; (3) are always innervated by two sensory cells with unbranched dendrites; and (4) typically exhibit undulating distal dendrites with conspicuous varicosities.

The fine structure of type-A trichoid sensilla in females is very similar to the long, pheromone-sensitive type-I trichoid sensilla of males (Fig. 1B; Keil, 1989; Lee and Strausfeld, 1990; Sanes and Hildebrand, 1976) in that both: (1) are taller than type-B trichoid sensilla of females or type-II trichoid sensilla of males (Keil, 1989; Lee and Strausfeld, 1990; Sanes and Hildebrand, 1976); (2) have cuticular shafts with a similar base diameter; (3) have cuticular walls that are thinner than those of type-B trichoid sensilla or type-II trichoid sensilla; (4) have similar transverse plates on the cuticular shaft that are pitted by pores; (5) have pores that are each associated with a similar number of pore tubules that extend into the shaft lumen; and (6) are innervated by two sensory cells with unbranched distal dendrites. A conspicuous morphological feature that differentiates type-A trichoid sensilla from type-I trichoid sensilla, however, is their length; type-I trichoid sensilla are much longer than type-A trichoid sensilla (70-600  $\mu\text{m}$  vs. 34  $\mu\text{m}$ , respectively).

The fine structure of type-B trichoid sensilla of females is comparable to that of type-II trichoid sensilla of males (Keil, 1989; Lee and Strausfeld, 1990; Sanes and Hildebrand, 1976) in that both: (1) are shorter than the type-A trichoid and type-I trichoid sensilla; (2) are similar in length; (3) have a similar base diameter; (4) have a wall thickness similar to that of type-A trichoid and type-I trichoid sensilla; and (5) have pores that are associated with a similar number of pore tubules that do not extend to the shaft lumen. Type-B trichoid sensilla can be distinguished from type-II trichoid sensilla with respect to innervation; the former sensillum type may be innervated by either one or three unbranched sensory neurons, whereas the latter type may be innervated by one, two, or three unbranched sensory cells.

Studies by Cuperus (1983) and Cuperus et al. (1983) revealed a sexual dimorphism with respect to the number of trichoid and basiconic sensilla in eleven species of small ermine moths (*Yponomeuta* spp). In later studies with moths of the same species, Cuperus (1985a, b) also showed a sexual dimorphism with respect to the number of sensory cells innervating the trichoid sensilla and number of pores present in both trichoid and basiconic sensilla. Cuperus (1985a) suggested that the fewer number of pores present in the trichoid sensilla of females of three lepidopteran species, as compared with those of males, could possibly account for the fact that these sensilla are at least ten to one hundred times less sensitive to sex attractants (see Den Otter et al., 1978; Van der Pers and Den Otter, 1978).

### Types-A and -B Basiconic Sensilla

There are two types of basiconic sensilla, type-A and type-B. Both are single-walled, multiporous sensilla that have the appearance of pegs (Figs. 1D, 2A). The type-B basiconic sensillum is reconstructed in a longitudinal view in Figure 7B. The type-A basiconic sensillum averages 22  $\mu\text{m}$  in length, has a diameter of 2  $\mu\text{m}$  near its base, and tapers to 0.65  $\mu\text{m}$  at its tip (Figs. 2A, 3A). The shaft wall averages 0.25  $\mu\text{m}$  in thickness (Fig. 3E) and is perforated by 58 pores per  $\mu\text{m}^2$ . Each pore averages 0.04  $\mu\text{m}$  in diameter (Fig. 3B). They are distributed in oblique, linear rows along the axis of the sensillum that extend to its tip (Fig. 3B). Five to eight pore tubules extend from the base of a small pore kettle and do not enter the lumen of the shaft. These sensilla are innervated by three sensory cells (Table 1). The dendrites emerge from the end of the dendritic sheath, near the base of the sensillum and divide into 7-9 branches (Fig. 3E). The branches ramify near the base of the sensillum and become tightly enclosed by the dendritic sheath.

The type-B basiconic sensillum averages 15  $\mu\text{m}$  in length, has a diameter of 1.6  $\mu\text{m}$  near its base, and tapers to 1.1  $\mu\text{m}$  at its tip (Figs. 1D, 2A, 3C). The shaft wall averages 0.13  $\mu\text{m}$  in thickness (Fig. 3F) and is perforated by 80 pores per  $\mu\text{m}^2$ . Pores average 0.03  $\mu\text{m}$  in diameter (Fig. 3D) and extend to the tip of the sensillum. They are arranged in oblique linear rows along the base of deep furrows. The majority of these furrows extend along the axis of the sensillum (Fig. 3D). Ten to twelve pore tubules travel from the base of a large pore kettle and appear to



be in direct contact with the distal dendritic branches. This sensillum has 40-50 branched distal dendrites (Fig. 3F). These dendrites emerge from the end of the dendritic sheath, near the base of the sensillum. The branches ramify near the base of the sensillum and become tightly enclosed by the dendritic sheath. Both types of basiconic sensilla are innervated by three sensory cells and are associated with three sheath cells (thecogen, trichogen, tormogen) (see Fig. 7B, Table 1).

The fine structure of the basiconic sensilla of female *M. sexta* most closely resembles that of the large basiconic sensilla of female and male *B. mori* (Steinbrecht, 1973,1980;Steinbrecht and Gnatzy, 1984), males of *M. sexta* (Keil, 1989;Lee and Strausfeld, 1990), *A. polyphemus* (Keil, 1984a), *A. pernyi* (Keil, 1984a), and *Y. vigintipunctatus* and *A. orana* (Cuperus, 1985a).

Basiconic sensilla can be distinguished from trichoid sensilla in that they (1) are shorter; (2) have a thinner cuticular wall that is pitted by a higher density of pores; (3) have a larger number of pore tubules associated with each pore; and (4) have many distal dendritic branches (Keil and Steinbrecht, 1984).

The fine structure of type-A and -B basiconic sensilla of female *M. sexta* closely resembles that of type-II basiconic and type-I basiconic, respectively, in males (Keil, 1989; Lee and Strausfeld, 1990; Sanes and Hildebrand, 1976). Both types in each sex have: (1) similar base diameters; (2) similar pore densities; (3) similar shaft thicknesses; (4) comparable numbers of pore tubules associated with each pore that extend into the shaft lumen; and (5) similar numbers of distal dendritic branches.

Comparisons between type-A and type-II basiconic sensilla and between type-B and type-I basiconic sensilla reveal a sexual dimorphism. Type-I basiconic sensilla of males: (1) are longer; (2) have a wider base diameter; and (3) typically are innervated by either two or three sensory cells with branched dendrites. Type-II basiconic sensilla of males: (1) are shorter and (2) are typically innervated by one, two, or three branched sensory cells. In contrast, both types of basiconic sensilla of females are innervated by three sensory cells with branched dendrites.

The basiconic sensilla of female *A. orana* (Den Otter et al., 1978) and *Yponomeuta* species (Van der Pers, 1981) are reported to be sensitive to plant odors, as are similar sensilla of both sexes of *B. mori* and male *A. pernyi* and *Sphinx pinastri* (see Schneider and Steinbrecht, 1968). The two types of basiconic sensilla of female *M. sexta* were not physiologically characterized. Based on their similarity to morphologically or physiologically characterized female olfactory basiconic sensilla of other insects, these sensilla of female *M. sexta* may also be olfactory and possess sensory cells tuned to plant odors.

### Auriculate Sensilla

The auriculate sensillum is single-walled, multiporous, and resembles an ear or spoon (Fig. 4A,B) and is reconstructed in a longitudinal view in Figure 7C. These sensilla rest in shallow depressions and extend only slightly above the level of the microtrichia (Fig. 4A-C). They are not clearly visible from the antennal surface. The upper surface of this sensillum is deeply, concavely indented (Fig. 4A,B). This sensillum averages 4-5  $\mu\text{m}$  in length and 4  $\mu\text{m}$  in diameter at its base (Fig. 4A,B). The shaft wall averages 0.07  $\mu\text{m}$  in thickness and is perforated by many pores averaging 0.04  $\mu\text{m}$  in diameter (Fig. 4D). Twelve to sixteen pore tubules extend from the base of a large pore and some appear to be in direct contact with the distal branches of the dendrites (Fig. 4E). The distal dendrites emerge from the end of the dendritic sheath, near the base of the sensillum and divide into 50-60 branches (Fig. 4D). Near the base of the sensillum, the branches ramify and become tightly enclosed by the dendritic sheath. These sensilla are

innervated by two sensory cells (see Fig. 7C; Table 1) with branched distal dendrites and are associated with three sheath cells (thecogen, trichogen, tormogen) (Fig. 4F, Table 1).

The most striking features of this sensillum type are the extremely thin cuticular wall, the perforation of this wall by a very large number of pores, the pore tubules that project into the lumen of the sensillum, and the numerous distal dendritic branches. Auriculate sensilla have been described by several authors, including both sexes of adult *Adoxophyes orana* (“rabbit’s ear-shaped sensilla” or “sensillum auricularia”; Den Otter et al., 1978), *Trichoplusia ni* (“sensilla auricillica”; Mayer et al., 1981), *Agrotis segetum* (“SW3” and “sickle-shaped”; Hallberg, 1981), and *Ostrinia nubilalis* (“sensilla auricillica”; Hallberg et al., 1994). The fine structure of auriculate sensilla of female *M. sexta* most closely resembles that of *A. orana* (Den Otter et al., 1978). The similarity of this sensillum type to morphologically or physiologically characterized auriculate sensilla of other insects suggests that this sensillum of female *M. sexta* may also be olfactory and have sensory cells tuned to plant odors.

### Type-A Coeloconic Sensilla

This sensillum is double-walled, multiporous, and resembles a peg recessed in a pit (Figs. 1D, 2A, 5A-C) and is depicted in a longitudinal view in Figure 7D. It averages 2  $\mu\text{m}$  in length and 2  $\mu\text{m}$  in diameter at the base (Fig. 5B). The rim of the pit averages 3.8  $\mu\text{m}$  in diameter (Fig. 5A,C) and seven to ten cuticular spines or “teeth” form a fringe around the peg. This sensillum comprises two distinct parts: a longitudinally grooved apical section and a smooth basal section that gradually tapers toward the apex (Fig. 5B). The apical section is scalloped and typically bears about 15-16 longitudinal grooves (Fig. 5B,D), which extend from just above the base to just below the tip of the sensillum. A bulbous extension, possibly resulting from the convergence of two or more ridges, is often apparent at the tip of the sensillum (Fig. 5B). Very small cuticular pores, found at the bottom of each groove, make a connection with the inside of the sensillum via cuticular spoke channels rather than pore tubules (Fig. 5B).

Each type-A coeloconic sensillum possesses double, concentric walls: the outer wall is scalloped or fluted with longitudinal grooves (Fig. 5D-F) and the inner wall is smooth and surrounds the distal dendrites (Fig. 5F) from the tip of the sensillum to near the base of the peg. The two walls are connected by cuticular spokes and within each spoke, a radial spoke channel extends from the inner lumen to one of the grooves (Fig. 5E). At this site, the spoke channel merges into the groove channel, which runs longitudinally at the bottom of each groove. The groove channels contain sensillar sinus liquor, since they are continuous with the spoke channels and with the inner lumen of the sensillum. The spoke channels are often filled with a conspicuous, electron-dense material from the sensillar sinus liquor (Fig. 5E). The electron-dense material is also found in lumina between the inner and outer cuticular walls (Fig. 5E) and is similar in appearance to that found in the sensillar sinus. The liquor from the sensillar sinus bathes 7-11 distal dendritic branches that extend to the tip of the sensillum. These branches emerge from the termination of the dendritic sheath, near the base of the sensillum (Fig. 5F) and have ramifications distal to the ciliary region (Fig. 5G). These sensilla are innervated by five sensory cells with branched distal dendrites and are associated with three sheath cells, the thecogen, trichogen, and tormogen cells (see Fig. 7D, Table 1).

The fine structure of type-A coeloconic sensilla of female *M. sexta* closely resembles that of sensilla of the same type in both sexes of *A. orana* (Den Otter et al., 1978), as well as the type-I coeloconic sensilla of male *M. sexta* (Lee and Strausfeld, 1990). In male *M. sexta*, these sensilla have been referred to as “sensilla coeloconica” (Sanes and Hildebrand, 1976), and “coeloconicum type-I” (Lee and Strausfeld, 1990). Similar coeloconic sensilla have also been described in other insects, such as *Arenivaga* species (Hawke and Farley, 1971a,b), *Simulium* species (Mercer and McIver, 1973), *Aedes aegypti* (McIver, 1974), *Anopheles stephensi* (Boo and McIver, 1976), *Tenebrio molitor* (Harbach and Larsen, 1977), *Periplaneta*

*americana* (Altner et al., 1977), *Locusta migratoria* (Altner et al., 1981), *Hypera postica* (Bland, 1981), *O. nubilalis* (Hallberg et al., 1994) and *B. mori* (Hunger and Steinbrecht, 1998).

This sensillum type possesses a double-wall with longitudinal grooves and spoke channels instead of pore tubules. Typically, double-walled, multiporous sensilla are exclusively olfactory, but some of these sensilla may also contain a single, cold-sensitive sensory cell (bimodal thermo-olfactory sensilla; Altner et al., 1977).

Double-walled, multiporous sensilla have been reported to be sensitive to fatty acids (Altner et al., 1981; Lacher, 1967), essential oils (Lacher, 1967), leaf extracts (Cuperus, 1985a; Den Otter et al., 1978; discussed in Schneider and Steinbrecht, 1968), water vapor, ammonia, acetone, acetic acid, anisole (Kellogg, 1970), amines (Altner et al., 1977), lactic acid (Davis, 1977), cyclic terpenoids (Klein et al., 1988), and polar aliphatic acids and aldehydes with shorter chain lengths (between 3 and 10 carbon atoms, such as hexanoic acid or heptanal) (Pophof, 1997; see also Altner et al., 1977). Like double-walled coeloconic sensilla of other insects, these sensilla of female *M. sexta* are likely to be olfactory and to possess sensory cells responsive to plant odors.

### Type-B Coeloconic and Styliform Complex Sensilla

The type-B coeloconic sensillum is single-walled, aporous, and has the appearance of a peg set on the floor of a pit (Fig. 6A,B). It is depicted in longitudinal view in Figure 7E. It averages 2  $\mu\text{m}$  in length and 2  $\mu\text{m}$  in diameter at its base (Fig. 6A). The rim of the pit averages 5.6  $\mu\text{m}$  in diameter (Fig. 6A,B). The dendritic channel runs centrally in the peg (Fig. 6C) and ends at the terminal molting pore. This pore is typically plugged proximally with electron-dense material. A single, unbranched distal dendrite ends near the tip of the peg, at the apex of the dendritic channel. A second distal dendrite ends slightly proximal to the first (Fig. 6C). Both of these dendrites completely fill the peg lumen and are tightly enclosed by a thick, dense dendritic sheath (Fig. 6C). The dendritic sheath isolates the dendrites within the dendritic channel from the surrounding cuticular pore canal system (Fig. 6C). It extends from near the plug at the apex of the sensillum to just distal of the ciliary region. A thicker, more electron-dense layer surrounds the dendritic sheath (Fig. 6C). A third distal dendrite ends near the base of the peg, forms membranous lamellae, and joins the other two dendrites. This dendrite reassumes a typical dendritic profile just distal to the ciliary region. These sensilla are innervated by three sensory cells and are associated with three sheath cells (thecogen, trichogen, and tormogen cells) (Fig. 7E, Table 1).

The styliform complex sensillum is single-walled, aporous, and resembles a peg and is depicted in longitudinal view in Figure 7F. It averages 38-40  $\mu\text{m}$  in length and is 14  $\mu\text{m}$  in width (Fig. 6D,E). It occurs singly on each annulus, is the largest type of sensillum on the antenna, and is positioned on the leading surface near the distal margin (Fig. 1A-C). It stands erect on the antennal surface and is surrounded mainly by type-A trichoid sensilla (Fig. 6D). The peg houses several, similar, contiguous sensilla (Fig. 6F), the number varying according to the location of the peg along the flagellum. Four to seven papillae are present at the tip of the sensillum (Fig. 6D) and indicate the number of sensilla that are housed within the peg. Each unit of the styliform complex sensillum is innervated by three sensory cells, two with large and cylindrical distal dendrites and one with a lamellate distal dendrite (Table 1). The distal dendritic bundles within each sensillum are individually enclosed by a thick dendritic sheath that extends from near the tip of the sensillum to just distal of the ciliary region (Fig. 6F). Each unit of the styliform complex sensillum is associated with three sheath cells, the thecogen, trichogen, and tormogen cells (Fig. 7F, Table 1). The fine structure of each unit of the styliform complex sensillum is very similar to that of type-B coeloconic sensilla.



The fine structure of the type-B coeloconic and styliform complex sensilla of female *M. sexta* closely resembles that of similar sensilla of male *M. sexta* (Lee and Strausfeld, 1990). In males, these sensilla have been referred to as “sensilla coeloconica” and “stubby peg” (Sanes and Hildebrand, 1976) and “coeloconicum type-II” and “sensillum styliform complex” (Lee and Strausfeld, 1990), respectively.

The external fine structure of these two sensillum types are very similar in that they: (1) lack pores and (2) are connected to the surrounding cuticle by an inflexible socket. Both type-B coeloconic sensilla and each unit of the styliform complex sensillum are also innervated by three sensory cells, two, long, voluminous distal dendrites tightly packed within the sensillum lumen that terminate near the tip of the sensillum (hygrosensory cell), and a short distal dendrite that terminates near the base of the sensillum and whose membrane displays infoldings (thermosensory cell) (Altner et al., 1983). This combination of sensory cell types has been referred to as a triad by Loftus (1976). The single thermosensory cell responds to a rapid fall (cold unit) in temperature, while the two antagonistic hygrosensory cells respond to a rapid rise (moist air unit) or fall (dry air unit) in humidity (Altner and Loftus, 1985). These hygrosensory cells respond to deformations of the cuticle of the sensillum (e.g., swelling) that exert mechanical forces on the dendritic membranes. Similar aporous sensilla were characterized as bimodal thermo-hygrosensilla by Yokohari (1981, 1983) and Altner et al. (1978, 1981). Aporous coeloconic sensilla have also been described in several insects, such as aphids (Bromley et al., 1979), grasshoppers (Altner et al., 1981; Ameismeier, 1985), walking sticks (Altner et al., 1978), and mosquitoes (Boo and McIver, 1975; McIver and Siemicki, 1979).

Aporous styliconic sensilla (similar to each unit of the styliform complex sensillum) have been described in several insects, such as ermine moths (Cuperus et al., 1983; Cuperus, 1985a,b; Van der Pers et al., 1980), silkmoths (Steinbrecht, 1989; Steinbrecht et al., 1989), turnip moths (Hallberg, 1981), saturniid moths (Zimmermann, 1991), and European cornborers (Hallberg et al., 1994).

The type-B coeloconic and styliform complex sensilla were not characterized physiologically. Based on analogous structures found in morphologically or physiologically characterized aporous coeloconic and styloconic sensilla found in other insects, these sensilla of female *M. sexta* are likely to be thermo-hygrosensitive and to possess sensory cells specialized to respond to fluctuations in temperature and humidity.

## DISTRIBUTION OF SENSILLA

The detailed inventory of the types and distribution of sensilla on a single annulus of a female antennal flagellum was based on a preparation of annulus 21 (counted from the base of the flagellum). This data is shown in Tables 2 and 3. The relative abundances of the various types of sensilla on this representative annulus are as follows (Table 3): type-A trichoid » type-A basiconic » type-B trichoid and type-B basiconic » auriculate and type-A coeloconic » type-B coeloconic and styliform complex.

Type-A trichoid sensilla are the main type of sensillum present and are most abundant along the distal and proximal margins of the leading, dorsal, and ventral surfaces of each annulus (Fig. 8A-C, open triangles). Along these margins, they are found in a band that is 2-3 sensilla deep. These bands merge toward the trailing surface and form a U-shaped cul-de-sac. This pattern is similar to, but less conspicuous than, the pattern of distribution of the male-specific trichoid sensilla (Lee and Strausfeld, 1990; see also Shields and Hildebrand, 1999a). In addition to their occurrence in these bands, they are also distributed over the three surfaces (leading, dorsal, and ventral; Fig. 8A-C; Table 2) and are most abundant on the dorsal surface in females. This feature is not found in males. Type-B trichoid (filled diamonds; Fig. 8D-F), types-A (open

circles; 8G-I) and -B basiconic (open diamonds Fig. 8D-F), auriculate (filled rectangles Fig. 8A-C), and type-A coeloconic (filled triangles Fig. 8G-I) sensilla are also distributed over the three surfaces. Type-B trichoid, types-A and -B basiconic, and type-A coeloconic sensilla are most abundant on the dorsal surface (Table 2). In addition, type-B coeloconic sensilla (Fig. 8I; filled circles) are found in very low number and only on the dorsal surface (Table 2). The auriculate sensilla are most abundant on the leading surface (Table 2). A single styliform complex sensillum is located on each annulus in the middle of the distal margin of the leading surface (Fig. 8A, filled star; Table 2).

The overall number of sensilla on each annulus is relatively similar between females and males (Table 3). A sexual dimorphism exists, however, with respect to the number of specific sensillum types on the three surfaces (Table 2). This feature is particularly prominent for type-A trichoid vs. type-I trichoid sensilla on the leading surface (287 vs. 54) and for type-B trichoid vs. type-II trichoid sensilla on the dorsal (123 vs. 315), ventral (59 vs. 315), and leading surfaces (64 vs. 106). In contrast, Mayer et al. (1981) found no sexual dimorphism with respect to the number of type-I trichoid sensilla of *T. ni* and only a slight difference between the sexes with respect to their distribution. They did find, however, a sexual dimorphism with respect to the number of type-II and type-III trichoid sensilla. In other studies, Cuperus (1983) and Cuperus et al. (1983) found no sexual dimorphism with respect to the types of antennal sensilla of some *Yponomeuta* species, but did find a marked difference in the distribution of various types of these sensilla (Cuperus et al., 1983).

Shields and Hildebrand (1999b) found that six of the seven types of sensilla (styliform complex not included) are most abundant on the dorsal surface of the female flagellum of *M. sexta*, (type-A trichoid, type-B trichoid, type-A basiconic, type-B basiconic, type-A coeloconic, and type-B coeloconic; Table 2). Lee and Strausfeld (1990), in contrast, found equal numbers of sensilla in male *M. sexta* on the ventral and dorsal surfaces (Table 2). The relative abundances of the seven types of antennal sensilla are similar in female and male *M. sexta* (Lee and Strausfeld, 1990; Table 3).

## ELECTROPHYSIOLOGICAL CHARACTERIZATION

### Type-A Trichoid Sensilla

Below, we describe the electrophysiological responses of type-A trichoid sensilla in response to a large panel of odorants (Fig. 9). Previous studies have shown that the trichoid sensilla in several species of female moths respond to hostplant volatiles (e.g., Anderson et al., 1995, 1996; Heinbockel and Kaissling, 1996; Priesner, 1979; Van der Pers, 1982). Two kinds of odor stimuli were used in this work (for materials and methods, see Shields and Hildebrand, 2001): purified synthetic volatile organic compounds and headspace volatiles from isolated plant material. The chemical purity of the organic compounds was assessed by gasliquid chromatography and fell in the range 95-99.9%. These odorants belonged to seven chemical classes and included terpenoids, aromatics, aliphatics, fatty-acid derivatives, a furan, N-bearing compounds, and greenleaf-volatile odorants, as well as mixtures of floral and vegetative headspace volatiles emitted by fragments of three hostplants of *M. sexta*.

Many of the odorants chosen represent floral headspace volatiles of native, night-blooming flowers, such as *Datura wrightii* (jimson weed), *Hymenocallis sonorensis* (spider lily), and *Oenothera caespitosa* (evening primrose), to which *M. sexta* and other hawkmoths are attracted for nectar-feeding (Knudsen and Tollsten, 1993; Raguso et al., 1996; Raguso and Light, 1998; Raguso and Willis, 1997). Also included in the panel of odorants are compounds that represent volatiles emitted by vegetation of solanaceous plants, such as *Lycopersicon* (tomato) (Andersen et al., 1988) and *Nicotiana* (tobacco) species (Buttery et al., 1987a,b), which are among the preferred hostplants of female *M. sexta* for oviposition (Yamamoto et al., 1969).

Knudsen and Tollsten (1993) reported that flowers having a “white floral” scent, such as that associated with many nightblooming moth-pollinated flowers, possess acyclic terpene alcohols (e.g., linalool, nerolidol, and farnesol), as well as the corresponding hydrocarbons, aromatic alcohols, and esters derived from them, in addition to esters of salicylic acid. Various plant-associated odorants, such as green-leaf volatiles (mainly saturated and unsaturated C<sub>6</sub> alcohols and aldehydes), terpenoids, and benzenoid compounds, are thought to play an important role in the attraction of insects to, and their recognition of, their hostplants (e.g., Boeckh, 1974; Gabel et al., 1992; Heath et al., 1992; Knudsen and Tollsten, 1993; Ma and Visser, 1978; Raguso and Light, 1998; Raguso and Willis, 1997; Renwick, 1989; Visser and Avé, 1978; Visser, 1979, 1986; Visser and Piron, 1995).

Of the 105 odor stimuli tested in this study, about 40% elicited no clear response from any of the ORCs from which recordings were obtained. These stimuli included: certain terpenoids (2-carene, *alpha*-pinene, *beta*-pinene, sabinene, ocimene, *trans*- $\beta$ -ocimene, limonene, *alpha*-terpinene, terpinolene, neryl acetone, *alpha*-humulene, *trans*-caryophyllene, *alpha*-cubebene, *beta*-elemene); aromatics (eugenol, isoeugenol, *m*-cresol, eugenol, methyleugenol, methylisoeugenol); aliphatic acids (butanoic, hexanoic, octanoic), esters (hexyl-2-methylbutyrate, methylacrylate), a diketone (2,3-butanedione), aldehydes (2,4-hexadienal, octanal, nonanal, decanal), and an alcohol (isopropanol); hydrocarbons (undecane, tridecane); N-bearing (1-nitropentane); O-heterocyclic (2-acetylfuran); sex-pheromone components (bombykal, C<sub>15</sub>); and, surprisingly, vegetative headspace-volatile mixtures from *Datura* and *Lycopersicon*. Likewise, foliage from *Nicotiana* plants did not evoke a response. Perhaps, these ORCs are sensitive to other odor stimuli that we have not tested in this study. The diluents used for plant-associated and pheromonal odorants (mineral oil and hexane, respectively), elicited no response in any of the sensilla tested.

### General Response Characteristics to Olfactory Stimulation

We have recorded from a total of 126 type-A trichoid sensilla by means of the cut-tip sensillum-recording technique (Kaissling, 1995; Shields and Hildebrand, 2001; Van der Pers and Den Otter, 1978). The responses of 35 ORCs associated with 31 sensilla (both ORCs were excited by odor stimulation in four sensilla) are summarized in Figure 9. The ORCs varied with respect to their background firing in the absence of applied stimuli. Usually, the unstimulated ORCs of all sensilla tested fired 1-3 spikes s<sup>-1</sup> (Figs. 10A, 11A), but some ORCs had higher background firing rates (9-12 spikes s<sup>-1</sup>; Fig. 10F). In a majority of sensilla, this background activity included two different spike amplitudes, which was interpreted to be due to firing of two ORCs as has been shown for various insect chemosensory sensilla (e.g., Anderson et al., 1995; de Bruyne et al., 1999; Getz and Akers, 1997). In 27 of the 31 sensilla, only one of the two ORCs in a sensillum was excited by stimulation with a particular odorant, while the other ORC exhibited no response or was inhibited. In some instances, in which a particular odorant elicited a robust response, the spike amplitude of the responding ORC gradually changed over the course of stimulation (Figs. 10D, 11B) as reported previously (Den Otter and Van der Goes van Naters, 1992; Guillet and Bernard, 1972; Rumbo, 1989). In the four sensilla in which both ORCs were excited by odor stimulation (Fig. 9, ORCs 6 and 34; 8 and 33; 9 and 30; 10 and 31), one ORC typically responded to terpenoids, while the other ORC responded mainly to aromatic, aliphatic, furan, or green-leaf odorants. When a complex blend of odorants (e.g., floral headspace, mainly terpenoid and aromatic volatiles from *Datura*) was tested, usually one or both of the ORCs of a sensillum responded with phasic-tonic excitation, with one ORC responding more strongly than the other (Fig. 10E).

### Classification of ORCs

Many researchers have classified ORCs based on their individual response profiles. Typically, terms such as “specialist” and “generalist” have been used to describe those ORCs. Specialist

ORCs have been defined as those responding with a high sensitivity and selectivity to a narrow range of related odorants or a single type of odor molecule, such as a pheromone component. Generalist ORCs have been classified as those responding with relatively lower sensitivity to a broad range of odorants, such as hostplant-derived volatiles (Schneider et al., 1964). It has been found, however, that some insect ORCs that respond to plant-associated odorants exhibit relatively high selectivity and sensitivity for effective stimulus molecules (e.g., Anderson et al., 1995; Heinbockel and Kaissling, 1996; Pophof, 1997; Priesner, 1979; Røsteliën et al., 2000a,b).

We have characterized the response profiles of ORCs of type-A trichoid sensilla of female *M. sexta* and have recognized three categories: (1) ORCs (9/35) that responded selectively to terpenoids, specifically certain oxygenated mono- and sesquiterpenoids such as linalool, geraniol, and *trans*-nerolidol (Fig. 9, ORCs 1-9; Fig. 10B-D); (2) ORCs (12/35) that responded exclusively to aromatics such as *cis*-3-hexenylbenzoate, 2-methylpropylbenzoate, ethyl-2-aminobenzoate, ethylsalicylate, and isoamylsalicylate (Fig. 9, ORCs 14-25, Fig. 11B-F); and (3) ORCs (14/35) that were strongly excited or inhibited by odorants belonging to two or more chemical classes, e.g., terpenoids, aromatics, aliphatics, green-leaf volatiles, a furan, and N-bearing volatiles (Fig. 9, ORCs 10-13, 26-35, Fig. 10G). Since the first two subsets responded to a narrow range of odorants, they were classified as “narrowly tuned” or having a narrow molecular receptive range (MRR; Mori and Shepherd, 1994). The third subset responded to a relatively broad range of odorants and was classified as “broadly tuned” or having a broad MRR. Among the latter subset of ORCs, there were several examples in which a particular odorant stimulated one ORC and inhibited another one (e.g., ORC 10 was activated by a terpenoid, whereas ORC 26 was inhibited by this odorant). In other cases, an individual ORC in a single sensillum was strongly activated by certain odorants but inhibited by others (e.g., ORC 26 was excited by ethylsalicylate and inhibited by guaiacol and ORC 27 was excited by 2-methylbutylbenzoate and inhibited by 3-octanol). Inhibitory responses were observed only in ORCs that had relatively high background firing rates (Fig. 10F). Both excitation and inhibition in response to some odorants have been reported in various insect sensilla, including individual ORCs in sensilla of the maxillary palps of *Drosophila melanogaster* (e.g., de Bruyne et al., 1999). These authors suggest that excitation and inhibition may reflect the depolarizing and hyperpolarizing ion currents in the ORCs. The existence of two modes of responses could allow multiple messages to be sent to the CNS by the same ORC, expanding the means by which odor coding is accomplished with a limited number of ORCs (de Bruyne et al., 1999).

Since the silkworm *B. mori* is a well-studied model for insect olfaction, several comparisons can be drawn from the present findings in *M. sexta* and those in *B. mori*: (1) The antenna of females of neither species is responsive to components of the female's sex pheromone at biologically significant concentrations (Boeckh et al., 1965; Schweitzer et al., 1976). In contrast, in female *Adoxophyes orana*, both sensory cells of the trichoid sensillum respond to the female sex pheromone (Den Otter et al., 1978). (2) Individual trichoid sensilla of female *B. mori* have an ORC that responds to 2,6-dimethyl-5-hepten-2-ol and linalool paired with an ORC that responds to benzoic acid and benzaldehyde (Heinbockel and Kaissling, 1996; Priesner, 1979). In some type-A trichoid sensilla of *M. sexta*, we found ORCs that responded strongly to benzoates but usually not to benzaldehyde (benzoic acid was not tested), and in other sensilla of the same morphological type, ORCs that respond strongly to terpenoids including linalool (2,6-dimethyl-5-hepten-2-ol was not tested). (3) The receptor cells of coeloconic sensilla of *B. mori*, like the receptor cells of type-A trichoid sensilla in *M. sexta*, are exclusively olfactory, exhibit both excitatory and inhibitory responses to different odorants, and have both broad and narrow MRRs (Pophof, 1997). The response patterns of ORCs of *B. mori* coeloconic sensilla, however, contrast sharply with the response patterns of ORCs of *M. sexta* type-A trichoid sensilla. We found that trichoid ORCs commonly are excited by terpenoids or aromatic esters and show no response to carboxylic acids or aldehydes (Shields

and Hildebrand, 2001), whereas coeloconic ORCs of *B. mori* were strongly excited by aliphatic carboxylic acids and aldehydes and either inhibited or unaffected by terpenoids.

### Sensitivities of ORCs

In another study (Shields and Hildebrand, 2001), the sensitivities of certain ORCs were characterized by taking the vapor pressures of odorants into consideration. There are only a few studies that have addressed this issue (e.g., Kafka, 1970, 1987; Kaissling, 1987, 1998; Visser, 1979). Because the partial pressure of an odorant in solution is directly proportional to the number of molecules  $\text{cm}^{-3}$  in the gaseous phase above the odorant solution, this number is proportional to the number of molecules striking the antenna when that gaseous phase is ejected from a syringe olfactometer (Alberly and Silbey, 1997; W.R. Salzman, personal communication). The sensitivities of ORCs were calculated by estimating the partial pressures of several odorants for which vapor-pressure data were available. The partial pressures of selected odorants were compared to the mean responses of the ORCs to the odorant in question and two main conclusions emerged: (1) some ORCs were much more sensitive to particular odorants than others, so that only a relatively small number of molecules were needed to elicit a strong response; and, importantly, (2) the most volatile odorants did not necessarily elicit the strongest responses (see Shields and Hildebrand, 2001).

### Temporal Characteristics of ORCs

The majority of ORCs tested gave phasic-tonic responses when stimulated by individual odorants (Figs. 10B-E, 11B-F). In a subset of ORCs, excitatory responses terminated relatively abruptly following odorant stimulation (e.g., Figs. 10B,C, 11C-E), a pattern apparently consistent with a decrease in odorant levels following the 200-ms odor-delivery period. In another subset of ORCs, some odorants always elicited a robust response that extended beyond the end of the odor-delivery period and then declined over one to several seconds to the background firing rate (e.g., Figs. 10D, 11B). Other examples of response types are given in Shields and Hildebrand (2001). Variations in temporal response characteristics have also been reported for antennal ORCs of several insect species (Almaas and Mustaparta, 1991; Almaas et al., 1991; Den Otter and Van der Goes van Naters, 1992; Heinbockel and Kaissling, 1996; Kaissling, 1987; Kaissling and Kramer, 1990; Rumbo and Kaissling, 1989).

### Neuronal Tracing and Mapping of ORC Axons

In insects, as in other invertebrates and vertebrates alike, the axons of ORCs project to and terminate in compartments of condensed synaptic neuropil, referred to as glomeruli, in the primary olfactory center in the CNS (Hildebrand and Shepherd, 1997). Mounting evidence indicates that the glomeruli are discrete anatomical and functional units. Each glomerulus is dedicated to collecting and processing olfactory information (about a subset of odor molecules) conveyed to that glomerulus by the axons of ORCs expressing particular olfactory receptor proteins (Buck, 1996; Buonviso and Chaput, 1990; Hildebrand and Shepherd, 1997; Mombaerts, 1996). A variety of experimental evidence, from studies using electrophysiological (e.g., Hansson et al., 1991; King et al., 2000; Mori and Yoshihara, 1995), activity-labeling and imaging (e.g., Friedrich and Korsching, 1997, 1998; Galizia et al., 1999; Hansson et al., 1992; Rodrigues and Buchner, 1984; Sharp et al., 1975), and molecular-biological methods (e.g., Mombaerts, 1996), supports the view that the arrays of glomeruli in the ALs of insects and the olfactory bulbs of vertebrates are organized chemotopically. This anatomical and neuronal organization is analogous to visuotopy of visual systems and tonotopy of auditory systems. Therefore, each olfactory glomerulus may represent an anatomical "address" from which the brain can extract information about specific molecular features of the olfactory environment (Christensen et al., 1996).



In *M. sexta*, the axons of antennal ORCs project via the antennal nerve to the ipsilateral AL. Here, they form synapses with processes of a subset of the approximately 1,200 central neurons in the AL (Camazine and Hildebrand, 1979; Homberg et al., 1988; Rössler et al., 1998, 1999). Each AL has 60 ordinary, sexually isomorphic glomeruli and three sexually dimorphic glomeruli in moths of both sexes (Rospars and Hildebrand, 2000). In males, there are three prominent glomeruli (cumulus, toroid 1, toroid 2), constituting the male-specific macroglomerular complex, that process information about the conspecific female's sex pheromone (Hansson et al., 1991; Heinbockel et al., 1999; Rospars and Hildebrand, 2000). In females, two of the homologous, sexually dimorphic glomeruli are referred to as the large female glomeruli (lateral and medial LFGs; Rössler et al., 1998, 1999; Rospars and Hildebrand, 2000). King et al. (2000) found that central neurons with arborizations in the lateral LFG respond preferentially to linalool and certain other monoterpenoids. They suggested that the LFGs may be involved in processing olfactory information that is important for the female's interactions with hostplants or courting males.

To reveal where the axons of the ORCs of trichoid type-A sensilla project in the AL of female *M. sexta*, we anterogradely labeled ORCs in groups of 5-10 sensilla on various surfaces of a single annulus located in the middle of an antennal flagellum with dextran-tetramethylrhodamine in each of 32 preparations. A majority of axonal projections from these ORCs terminated in the two LFGs located in the dorsolateral region of the ipsilateral AL, near the entrance of the antennal nerve into the AL (Fig. 12). In addition to the LFGs, some of the other 60 spheroidal, ordinary, sexually isomorphic glomeruli received sparse projections of a subset of ORC afferent axons.

Based on these anatomical findings and on our evidence that the ORCs of type-A trichoid sensilla are tuned mainly to terpenoids and aromatic esters, we hypothesize that information about odorants belonging to those chemical classes is processed in the LFGs (King et al., 2000; Shields and Hildebrand, 1999c, 2001).

#### ACKNOWLEDGMENTS

We are grateful to Dr. Thomas Heinbockel for critically reviewing this manuscript. We also thank Dr. Philippe Lucas for inviting us to write this review, David Bentley for technical assistance and use of the SEM, Gary Chandler and Sarah Biedrzycki for use and assistance of the FESEM, Dr. W. Salzman for advice about estimating the partial pressures of individual volatile compounds. Patricia Jansma for technical assistance with confocal microscopy, Drs. D.M. Light (USDA-ARS, Western Regional Research Center, Albany, CA) and R.A. Raguso (University of South Carolina) for generously providing many of the odorants tested, and Dr. A. A. Osman for rearing *Manduca sexta*. This work was supported by NIH grant DC-02751 to J.G.H. and a grant from the American Philosophical Society to V.D.S.

Contract grant sponsor: NIH; Contract grant number: DC-02751; Contract grant sponsor: American Philosophical Society.

#### REFERENCES

- Alberty, RA.; Silbey, RJ. Physical chemistry. 2nd ed.. Wiley; New York: 1997.
- Almaas TJ, Mustaparta H. *Heliothis virescens*: response characteristics of receptor neurons in sensilla trichodea type 1 and 2. *J Chem Ecol* 1991;17:953-972.
- Almaas TJ, Christensen TA, Mustaparta H. Chemical communication in heliothine moths. I. Antennal receptor neurons encode several features of intra- and interspecific odorants in the male corn earworm moth *Helicoverpa zea*. *J Comp Physiol A* 1991;169:249-258.
- Altner H, Loftus R. Ultrastructure and function of insect thermo- and hygrosensors. *Annu Rev Entomol* 1985;30:273-295.
- Altner H, Sass H, Altner I. Relationship between structure and function of antennal chemo-, hygro-, and thermoreceptive sensilla in *Periplaneta americana*. *Cell Tissue Res* 1977;176:389-405. [PubMed: 832305]

- Altner H, Tichy H, Altner I. Lamellated outer dendritic outer segments of a sensory cell within a poreless thermo- and hygroreceptive sensillum of the insect *Carausius morosus*. *Cell Tissue Res* 1978;191:287–304. [PubMed: 679268]
- Altner H, Routil Ch, Loftus R. The structure of bimodal chemo-, thermo-, and hygroreceptive sensilla on the antenna of *Locusta migratoria*. *Cell Tissue Res* 1981;215:289–308. [PubMed: 7214477]
- Altner H, Schaller-Selzer L, Stetter H, Wohlrab I. Poreless sensilla with inflexible sockets: a comparative study of a fundamental type of insect sensilla probably comprising thermo- and hygroreceptors. *Cell Tissue Res* 1983;234:279–307. [PubMed: 6196120]
- Ameisemeier F. Embryonic development and molting of the antennal coeloconic no pore- and double-walled wall pore sensilla in *Locusta migratoria* (Insecta, Orthopteroidea). *Zoomorphology* 1985;105:356–366.
- Andersen RA, Hamilton-Kemp TR, Loughrin JH, Hughes CG, Hildebrand DF, Sutton TG. Green leaf headspace volatiles from *Nicotiana tabacum* lines of different trichome morphology. *J Agric Food Chem* 1988;36:295–299.
- Anderson P, Hansson BS, Löfqvist J. Plant-odour-specific receptor neurones on the antennae of female and male *Spodoptera littoralis*. *Physiol Entomol* 1995;20:189–198.
- Anderson P, Larsson M, Löfqvist J, Hansson BS. Plant odour receptor neurones on the antennae of the two moths *Spodoptera littoralis* and *Agrotis segetum*. *Entomol Exp Appl* 1996;80:32–34.
- Bland RG. Antennal sensilla of the adult alfalfa weevil, *Hypera postica* (Gyllenhal) (Coleoptera: Curculionidae). *Int J Insect Morphol Embryol* 1981;10:265–274.
- Boo KS, McIver SB. Fine structure of sunken thick-walled pegs (sensilla ampullacea and coeloconica) on the antennae of mosquitoes. *Can J Zool* 1975;53:262–266. [PubMed: 1125869]
- Boo KS, McIver SB. Fine structure of surface and sunken grooved pegs on the antenna of female *Anopheles stephensi* (Diptera: Culicidae). *Can J Zool* 1976;54:235–244. [PubMed: 1253017]
- Boeckh J. Die Reaktionen Olfaktorischer Neurone im Deutocerebrum von Insekten im Vergleich zu den Antwortmustern der Geruchssinneszellen. *J Comp Physiol* 1974;90:183–205.
- Boeckh J, Tolbert LP. Synaptic organization and development of the antennal lobe in insects. *Microsc Res Tech* 1993;24:260–280. [PubMed: 8431606]
- Boeckh J, Kaissling KE, Schneider D. Insect olfactory receptors. *Cold Spring Harbor Symp Quant Biol* 1965;30:263–280. [PubMed: 5219480]
- Bromley AK, Dunn JA, Anderson M. Ultrastructure of the antennal sensilla of aphids: I. Coeloconic and placoid sensilla. *Cell Tissue Res* 1979;203:427–442. [PubMed: 519733]
- Buck LB. Information coding in the vertebrate olfactory system. *Annu Rev Neurosci* 1996;19:517–544. [PubMed: 8833453]
- Buonviso N, Chaput MA. Response similarity of odors in olfactory bulb output cells presumed to be connected to the same glomerulus: electrophysiological study using simultaneous singleunit recordings. *J Neurophysiol* 1990;63:447–454. [PubMed: 2329354]
- Buttery RG, Teranishi R, Ling LC. Fresh tomato aroma volatiles: a quantitative study. *J Agric Food Chem* 1987a;35:540–544.
- Buttery RG, Ling LC, Light DM. Tomato leaf volatile aroma odorants. *J Agric Food Chem* 1987b; 35:1039–1042.
- Camazine SM, Hildebrand JG. Central projections of antennal sensory neurons in mature and developing *Manduca sexta*. *Soc Neurosci Abstr* 1979;5:155.
- Christensen TA, Heinbockel T, Hildebrand JG. Olfactory information processing in the brain: encoding chemical and temporal features of odors. *J Neurobiol* 1996;30:82–91. [PubMed: 8727985]
- Cuperus PL. Distribution of antennal sense organs in male and female ermine moth, *Yponomeuta vigintipunctatus* (Retzius) (Lepidoptera: Yponomeutidae). *Int J Insect Morphol Embryol* 1983;12:59–66.
- Cuperus PL. Inventory of pores in antennal sensilla of *Yponomeuta* spp. (Lepidoptera: Yponomeutidae) and *Adoxophyes orana* F.v.R (Lepidoptera: Tortricidae). *Int J Insect Morphol Embryol* 1985a; 14:347–359.
- Cuperus PL. Ultrastructure of antennal sense organs of small ermine moths, *Yponomeuta* spp. (Lepidoptera: Yponomeutidae). *Int J Insect Morphol Embryol* 1985b;14:179–191.

- Cuperus PL, Thomas G, Den Otter CJ. Interspecific variation and sexual dimorphism of antennal receptor morphology, in European *Yponomeuta* (Latreille) (Lepidoptera: Yponomeutidae). *Int J Insect Morphol Embryol* 1983;12:67–78.
- Davis EE. Response of the antennal receptors of the male *Aedes aegypti* mosquito. *J Insect Physiol* 1977;23:613–617.
- de Bruyne M, Clyne PJ, Carlson JR. Odor coding in a model olfactory organ: the *Drosophila* maxillary palp. *J Neurosci* 1999;19:4520–4532. [PubMed: 10341252]
- Den Otter CJ, Schuil HA, Sander Van Oosten A. Reception of host-plant odours and female sex pheromone in *Adoxophyes orana* (Lepidoptera: Tortricidae): electrophysiology and morphology. *Entomol Exp Appl* 1978;24:370–378.
- Den Otter CJ, Van der Goes van Naters WM. Single cell recordings from tsetse (*Glossina m. morsitans*) antennae reveal olfactory mechano- and cold receptors. *Physiol Entomol* 1992;17:33–42.
- Ernst K-D. Die Feinstruktur von Riechsensillen auf der Antenne des Aäskafers *Necrophorus* (Coleoptera). *Z Zellforsch Mikrosk Anat* 1969;94:72–102. [PubMed: 5764098]
- Friedrich RW, Korsching SI. Combinatorial and chemotopic odorant coding in the zebrafish olfactory bulb visualized by optical imaging. *Neuron* 1997;18:737–752. [PubMed: 9182799]
- Friedrich RW, Korsching SI. Chemotopic, combinatorial, and noncombinatorial odorant representations in the olfactory bulb revealed using a voltage-sensitive axon tracer. *J Neurosci* 1998;18:9977–9988. [PubMed: 9822753]
- Gabel G, Thiéry D, Suchy V, Marion-Poll F, Hradsky P, Farkas P. Floral volatiles of *Tanacetum vulgare* L. attractive to *Lobesia botrana* (Den et Schiff.) females. *J Chem Ecol* 1992;18:693–701.
- Galizia CG, Sachse S, Rappert A, Menzel R. The glomerular code for odor representation is species specific in the honeybee *Apis mellifera*. *Nature Neurosci* 1999;2:473–478. [PubMed: 10321253]
- Getz WM, Akers RP. Response of American cockroach (*Periplaneta americana*) olfactory receptors to selected alcohol odorants and their binary combinations. *J Comp Physiol A* 1997;180:701–709.
- Guillet JC, Bernard J. Shape and amplitude of the spikes induced by natural or electrical stimulation in insect receptors. *J Insect Physiol* 1972;18:2155–2171.
- Hallberg E. Fine-structural characteristics of the antennal sensilla of *Agrotis segetum* (Insecta: Lepidoptera). *Cell Tiss Res* 1981;218:209–218.
- Hallberg E, Hansson BS, Steinbrecht RA. Morphological characteristics of antennal sensilla in the European cornborer *Ostrinia nubilalis* (Lepidoptera: Pyralidae). *Tissue Cell* 1994;26:489–502.
- Hansson BS. Olfaction in Lepidoptera. *Experientia* 1995;51:1003–1027.
- Hansson BS, Christensen TA, Hildebrand JG. Functional organization of the macroglomerular complex in the antennal lobe of the sphinx moth *Manduca sexta*. *J Comp Neurol* 1991;312:264–278. [PubMed: 1748732]
- Hansson BS, Ljungberg H, Hallberg E, Löfstedt C. Functional specialization of olfactory glomeruli in a moth. *Science* 1992;256:1313–1315. [PubMed: 1598574]
- Harbach RE, Larsen JR. Fine structure of antennal sensilla of the adult mealworm beetle, *Tenebrio molitor* L. (Coleoptera: Tenebrionidae). *Int J Insect Morphol Embryol* 1977;6:41–60.
- Hawke SD, Farley RD. Antennal chemoreceptors of the desert burrowing cockroach, *Arenivaga* sp. *Tissue Cell* 1971a;3:649–664.
- Hawke SD, Farley RD. The role of pore structures in the selective permeability of antennal sensilla of the desert burrowing cockroach, *Arenivaga* sp. *Tissue Cell* 1971b;3:665–674.
- Heath RR, Landolt PJ, Dueben B, Lenczewski B. Identification of floral compounds of night-blooming jessamine attractive to cabbage-looper moths. *Environ Entomol* 1992;21:854–859.
- Heinbockel T, Kaissling K-E. Variability of olfactory receptor neuron responses of female silkmoths (*Bombyx mori* L.) to benzoic acid and ( $\pm$ )-linalool. *J Insect Physiol* 1996;42:565–578.
- Heinbockel T, Christensen TA, Hildebrand JG. Temporal tuning of odor responses in pheromone-responsive projection neurons in the brain of the sphinx moth *Manduca sexta*. *J Comp Neurol* 1999;409:1–12. [PubMed: 10363707]
- Hildebrand JG. Olfactory control of behavior in moths: central processing of odor information and the functional significance of olfactory glomeruli. *J Comp Physiol A* 1996;178:5–19. [PubMed: 8568724]

- Hildebrand JG, Shepherd G. Mechanisms of olfactory discrimination: converging evidence for common principles across phyla. *Annu Rev Neurosci* 1997;20:595–631. [PubMed: 9056726]
- Hildebrand JG, Rössler W, Tolbert LP. Postembryonic development of the olfactory system in the moth *Manduca sexta*: primary afferent control of glomerular development. *Semin Cell Dev Biol* 1997;8:163–170. [PubMed: 15001092]
- Homberg U, Montague RA, Hildebrand JG. Anatomy of antenno-cerebral pathways in the brain of the sphinx moth *Manduca sexta*. *Cell Tissue Res* 1988;254:225–281. [PubMed: 2461804]
- Hunger T, Steinbrecht RA. Functional morphology of a double-walled multiporous olfactory sensillum: the sensillum coeloconicum of *Bombyx mori* (Insecta, Lepidoptera). *Tissue Cell* 1998;30:14–29.
- Kafka WA. Molekulare Wechselwirkungen bei der Erregung einzelner Riechzellen. *J Comp Physiol* 1970;70:105–143.
- Kafka WA. Similarity of reaction spectra and odor discrimination: single receptor cell recordings in *Antheraea polyphemus* (Saturniidae). *J Comp Physiol A* 1987;161:867–880.
- Kaissling, K-E. Sensory transduction in insect olfactory receptors. In: Jaenicke, L., editor. *Biochemistry of sensory functions*. Springer; New York: 1974. p. 243-273.
- Kaissling K-E. Chemo-electrical transduction in insect olfactory receptors. *Annu Rev Neurosci* 1986;9:121–145. [PubMed: 3518584]
- Kaissling, K-E. RH Wright lectures on insect olfaction. Col-bow, K., editor. Simon Fraser University; Burnaby, BC, Canada: 1987.
- Kaissling, K-E. Single unit and electroantennogram recordings in insect olfactory organs. In: Spielman, AI.; Brand, JG., editors. *Experimental cell biology of taste and olfaction. Current techniques and protocols*. CRC Press; New York: 1995. p. 361-377.
- Kaissling K-E. Flux detectors versus concentration detectors: two types of chemoreceptors. *Chem Senses* 1998;23:99–111. [PubMed: 9530975]
- Kaissling K-E, Kramer E. Sensory basis of pheromone-mediated orientation in moths. *Verh Dtsch Zool Ges* 1990;83:109–131.
- Keil TA. Contacts of pore tubules and sensory dendrites in antennal chemosensilla of a silkmoth: demonstration of a possible pathway for olfactory molecules. *Tissue Cell* 1982;14:451–462. [PubMed: 6890723]
- Keil TA. Reconstruction and morphometry of silkmoth olfactory hairs: a comparative study of sensilla trichodea on the antennae of male *Antheraea polyphemus* and *Antheraea pernyi* (Insecta, Lepidoptera). *Zoomorphology* 1984a;104:147–156.
- Keil TA. Surface coats of pore tubules and olfactory sensory dendrites of a silkmoth revealed by cationic markers. *Tissue Cell* 1984b;16:705–717. [PubMed: 6515640]
- Keil TA. Fine structure of the pheromone-sensitive sensilla on the antenna of the hawkmoth, *Manduca sexta*. *Tissue Cell* 1989;21:139–151.
- Keil, TA.; Steinbrecht, RA. Mechanosensitive and olfactory sensilla of insects. In: King, RC.; Akai, H., editors. *Insect ultrastructure*. 2. Plenum; New York: 1984. p. 477-516.
- Kellogg FE. Water vapor and carbon dioxide receptors in *Aedes aegypti* (L.). *J Insect Physiol* 1970;16:99–108. [PubMed: 5417711]
- Klein U, Bock C, Kafka WA, Moore TE. Antennal sensilla of *Magicicada cassini* (Fisher) (Homoptera: Cicadidae): fine structure and electrophysiological evidence for olfaction. *Int J Insect Morphol Embryol* 1988;17:153–167.
- Knudsen JT, Tollsten L. Trends in floral scent chemistry in pollination syndromes: floral scent composition in moth-pollinated taxa. *Bot J Linn Soc* 1993;113:263–284.
- Lacher V. Elektrophysiologische Untersuchungen an einzelnen Geruchsrezeptoren auf den Antennen weiblicher Moskitos (*Aedes aegypti* L.). *J Insect Physiol* 1967;13:1461–1470. [PubMed: 6077610]
- Lee JK, Strausfeld NJ. Structure, distribution and number of surface sensilla and their receptor cells on the olfactory appendage of the male moth, *Manduca sexta*. *J Neurocytol* 1990;19:519–538. [PubMed: 2243245]
- Loftus R. Temperature-dependent dry receptor on antenna of *Periplaneta*. Tonic response. *J Comp Physiol* 1976;111:153–170.

- Ma W-C, Visser JH. Single unit analysis of odour quality coding by the olfactory antennal receptor system of the Colorado beetle. *Entomol Exp Appl* 1978;24:320–333.
- Mayer MS, Mankin RW, Carlisle TC. External antennal morphometry of *Trichoplusia ni* (Hübner) (Lepidoptera: Noctuidae). *Int J Insect Morphol Embryol* 1981;10:185–201.
- McIver S. Fine structure of antennal grooved pegs of the mosquito, *Aedes aegypti*. *Cell Tissue Res* 1974;153:327–337. [PubMed: 4458949]
- McIver S, Siemicki R. Fine structure of antennal sensilla of male *Aedes aegypti* (L.). *J Insect Physiol* 1979;25:21–28.
- Mechaber WL, Hildebrand JG. Novel, non-solanaceous hostplant record for *Manduca sexta* (Lepidoptera: Sphingidae) in the southwestern United States. *Ann Ent Soc Am* 2000;93:447–451.
- Mercer KL, McIver SB. Studies on the antennal sensilla of selected blackflies (Diptera: Simuliidae). *Can J Zool* 1973;51:729–734. [PubMed: 4756149]
- Metcalf RL. Plant volatiles as insect attractants. *CRC Crit Revs Plant Scis* 1987;5:251–301.
- Mombaerts P. Targeting olfaction. *Curr Opin Neurobiol* 1996;6:481–486. [PubMed: 8794106]
- Mori K, Shepherd GM. Emerging principles of molecular signal processing by mitral/tufted cells in the olfactory bulb. *Semin Cell Biol* 1994;5:65–74. [PubMed: 8186397]
- Mori K, Yoshihara Y. Molecular recognition and olfactory processing in the mammalian olfactory system. *Prog Neurobiol* 1995;45:585–619. [PubMed: 7624486]
- Oland LA, Tolbert LP. Effects of hydroxyurea parallel the effects of radiation in developing olfactory glomeruli. *J Comp Neurol* 1988;27:377–387. [PubMed: 3216049]
- Oland LA, Tolbert LP. Patterns of glial proliferation during formation of olfactory glomeruli in an insect. *Glia* 1989;2:10–24. [PubMed: 2523336]
- Pophof B. Olfactory responses recorded from sensilla coeloconica of the silkworm *Bombyx mori*. *Physiol Entomol* 1997;22:239–248.
- Priesner E. Progress in the analysis of pheromone receptor systems. *Ann Zool Ecol Anim* 1979;11:533–546.
- Raguso RA, Light DM. Electroantennogram responses of male *Sphinx perelegans* hawkmoths to floral and “green-leaf volatiles”. *Entomol Exp Appl* 1998;86:287–293.
- Raguso RA, Willis MA. Floral scent and its role(s) in hawkmoth attraction. *Chem Senses* 1997;22:774–775.
- Raguso RA, Light DM, Pichersky E. Electroantennogram response of *Hyles lineata* (Sphingidae: Lepidoptera) to volatile odorants from *Clarkia breweri* (Onagraceae) and other moth-pollinated flowers. *J Chem Ecol* 1996;22:1735–1766.
- Ramaswamy SB. Host finding by moths: sensory modalities and behaviours. *J Insect Physiol* 1988;34:235–249.
- Renwick JAA. Chemical ecology of oviposition in phytophagous insects. *Experientia* 1989;45:223–228.
- Roche-King J, Christensen TA, Hildebrand JG. Response characteristics of an identified, sexually dimorphic olfactory glomerulus. *J Neurosci* 2000;20:2391–2399. [PubMed: 10704513]
- Rodrigues V, Buchner E. [<sup>3</sup>H]2-deoxyglucose mapping of odor-induced neuronal activity in the antennal lobes of *Drosophila melanogaster*. *Brain Res* 1984;324:374–378. [PubMed: 6442179]
- Rospars JP, Hildebrand JG. Sexually dimorphic and isomorphic glomeruli in the antennal lobes of the sphinx moth *Manduca sexta*. *Chem Senses* 2000;25:119–129. [PubMed: 10781018]
- Rössler W, Tolbert LP, Hildebrand JG. Early formation of sexually dimorphic glomeruli in the developing olfactory lobe of the brain of the moth *Manduca sexta*. *J Comp Neurol* 1998;396:415–428. [PubMed: 9651002]
- Rössler W, Randolph PW, Tolbert LP, Hildebrand JG. Axons of olfactory receptor cells of transsexually grafted antennae induce development of sexually dimorphic glomeruli in *Manduca sexta*. *J Neurobiol* 1999;38:521–541. [PubMed: 10084687]
- Røsteliën T, Borg-Karlson A-K, Mustaparta H. Selective receptor neurone responses to *E*- $\beta$ -ocimene,  $\beta$ -myrcene, *E,E*- $\alpha$ -farnesene and *homo*-farnesene in the moth *Heliothis virescens*, identified by gas chromatography linked to electrophysiology. *J Comp Physiol A* 2000a;186:833–847.



- Røstelien T, Borg-Karlson A-K, Fäldt J, Jacobsson U, Mustaparta H. The plant sesquiterpene germacrene D specifically activates a major type of antennal receptor neuron of the tobacco budworm moth *Heliothis virescens*. *Chem Senses* 2000b;25:141–148.
- Rumbo ER. The shape of extracellularly recorded nerve impulses from pheromone receptors. *Chem Senses* 1989;14:361–369.
- Rumbo ER, Kaissling K-E. Temporal resolution of odor pulses by three types of pheromone receptor cells in *Antheraea polyphemus*. *J Comp Physiol A* 1989;165:281–291.
- Sanes JR, Hildebrand JG. Structure and development of antennae in a moth, *Manduca sexta*. *Dev Biol* 1976;51:282–299.
- Schneider D, Steinbrecht RA. Checklist of insect olfactory sensilla. *Symp Zool Soc London* 1968;23:279–297.
- Schneider D, Lacher V, Kaissling K-E. Die Reaktionsweise und Reaktionsspektrum von Riechzellen bei *Antheraea pernyi* (Lepidoptera, Saturniidae). *Z Vergl Physiol* 1964;48:632–662.
- Schweitzer ES, Sanes JR, Hildebrand JG. Ontogeny of electroantennogram responses in the moth *Manduca sexta*. *J Insect Physiol* 1976;22:955–960. [PubMed: 947988]
- Sharp FR, Kauer JS, Shepherd GM. Local sites of activity-related glucose metabolism in rat olfactory bulb during olfactory stimulation. *Brain Res* 1975;98:596–600. [PubMed: 1182541]
- Shields VDC, Hildebrand JG. Fine structure of antennal sensilla of the female sphinx moth, *Manduca sexta* (Lepidoptera: Sphingidae). I. trichoid and basiconic sensilla. *Can J Zool* 1999a;77:290–301.
- Shields VDC, Hildebrand JG. Fine structure of antennal sensilla of the female sphinx moth, *Manduca sexta* (Lepidoptera: Sphingidae). II. auriculate, coeloconic, and styliform complex sensilla. *Can J Zool* 1999b;77:302–313.
- Shields VDC, Hildebrand JG. Responses from the olfactory receptor cells of trichoid sensilla on the antenna of the female sphinx moth, *Manduca sexta*. *Soc Neurosci Abstr* 1999c;25:124.
- Shields VDC, Hildebrand JG. Responses of a population of antennal olfactory receptor cells in the female moth *Manduca sexta* to plant-associated volatile organic compounds. *J Comp Physiol A* 2001;186:1135–1151. [PubMed: 11288825]
- Slifer EH, Prestage JJ, Beams HW. The chemoreceptors and other sense organs on the antennal flagellum of the grasshopper (Orthoptera: Acrididae). *J Morphol* 1959;105:145–191. [PubMed: 13831667]
- Steinbrecht RA. Der Feinbau olfaktorischer Sensillen des Seidenspinners (Insecta, Lepidoptera). Rezeptorfortsätze und reizleitender Apparat. *Z Zellforsch* 1973;139:533–565. [PubMed: 4724530]
- Steinbrecht RA. Cryofixation without cryoprotectants. Freeze substitution and freeze etching of an insect olfactory receptor. *Tissue Cell* 1980;12:73–100. [PubMed: 6987774]
- Steinbrecht RA. The fine structure of thermo-/hygrosensitive sensilla in the silkworm *Bombyx mori*: receptor membrane substructure and sensory cell contacts. *Cell Tissue Res* 1989;255:49–57.
- Steinbrecht RA, Müller B. On the stimulus conducting structures in insect olfactory receptors. *Z Zellforsch* 1971;117:570–575. [PubMed: 5088155]
- Steinbrecht RA, Gnatzy W. Pheromone receptors in *Bombyx mori* and *Antheraea pernyi*. I. Reconstruction of the cellular organization of the sensilla trichodea. *Cell Tissue Res* 1984;235:25–34. [PubMed: 6697381]
- Steinbrecht RA, Lee J-K, Altner H, Zimmermann B. Volume and surface of receptor and auxiliary cells in hygro-/thermoreceptive sensilla of moths (*Bombyx mori*, *Antheraea pernyi*, and *A. polyphemus*). *Cell Tissue Res* 1989;255:59–67.
- Van der Pers JNC. Comparison of electroantennogram response spectra to plant volatiles in seven species of *Yponomeuta* and in the tortricid *Adoxophyes orana*. *Entomol Exp Appl* 1981;30:181–192.
- Van der Pers JNC. Comparison of single cell responses of antennal sensilla trichodea in the nine European small ermine moths (*Yponomeuta* spp.). *Entomol Exp Appl* 1982;31:225–264.
- Van der Pers JNC, Den Otter CJ. Single cell responses from olfactory receptors of small ermine moths, *Yponomeuta* spp. (Lepidoptera: Yponomeutidae). *Int J Insect Morphol Embryol* 1978;9:15–23.
- Van der Pers JNC, Cuperus PL, Den Otter CJ. Distribution of sense organs on male antennae of small ermine moths, *Yponomeuta* spp. (Lepidoptera: Yponomeutidae). *Int J Insect Morphol Embryol* 1980;9:15–23.

- Visser JH. Electroantennogram responses of the Colorado beetle, *Leptinotarsa decemlineata*, to plant volatiles. *Entomol Exp Appl* 1979;25:86–97.
- Visser JH. Host odor perception in phytophagous insects. *Annu Rev Entomol* 1986;31:121–144.
- Visser JH, Avé DA. General green leaf volatiles in the olfactory orientation of the Colorado beetle, *Leptinotarsa decemlineata*. *Entomol Exp Appl* 1978;24:538–549.
- Visser JH, Piron PGM. Olfactory antennal responses to plant volatiles in apterous virginoparae of the vetch aphid *Megoura viciae*. *Entomol Exp Appl* 1995;77:37–46.
- Vogt, RG. The molecular basis of pheromone reception: its influence on behavior. In: Prestwich, GD.; Blomquist, GJ., editors. *Pheromone biochemistry*. Academic Press; New York: 1987. p. 385-431.
- Vogt RG, Riddiford LM. Pheromone binding and inactivation by moth antennae. *Nature* 1981a;293:161–163. [PubMed: 18074618]
- Vogt, RG.; Riddiford, LM.; Sehna, F.; Zabza, A.; Menn, JJ.; Cymborowski, B. Regulation of insect development and behavior. Polytechnical Univ Press; Poland: 1981b. Pheromone deactivation by antennal proteins of Lepidoptera; p. 955-967.
- Vogt, RG.; Riddiford, LM. Pheromone reception: a kinetic equilibrium. In: Payne, TL.; Birch, M.; Kennedy, CEJ., editors. *Mechanisms in insect olfaction*. Oxford Univ Press; New York: 1986. p. 201-208.
- Yamamoto RT, Jenkins RY, McClusky RK. Factors determining the selection of plants for oviposition by the tobacco hornworm, *Manduca sexta*. *Entomol Exp Appl* 1969;12:504–508.
- Yokohari F. The sensillum capitulum, an antennal hygroand thermoreceptive sensillum of the cockroach, *Periplaneta americana* L. *Cell Tissue Res* 1981;216:525–543. [PubMed: 7237519]
- Yokohari F. The coelocapitular sensillum, an antennal hygro- and thermoreceptive sensillum of the honey bee, *Apis mellifera* L. *Cell Tissue Res* 1983;233:355–365. [PubMed: 6616572]
- Zimmermann B. Differentiation of the thermo-/hygrosensitive (no-pore) sensilla on the antenna of *Antheraea pernyi* (Lepidoptera, Saturniidae): a study of cryofixed material. *Cell Tissue Res* 1991;266:427–440.

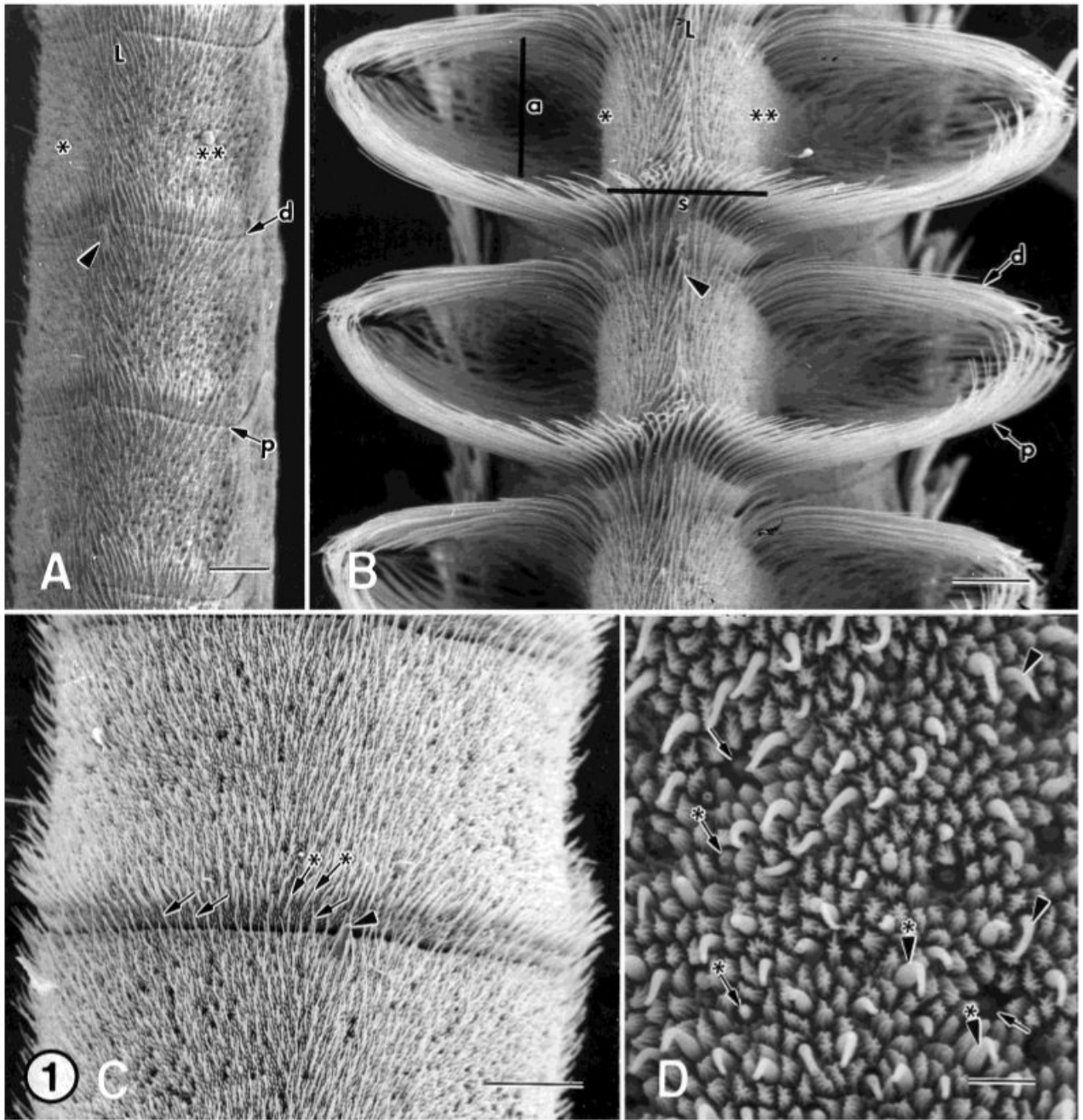


**Fig. 1.**

**A:** SEM of three adult female antennal flagellar annuli. Flagellum is turned slightly ventral. Bordering each side of the leading surface (L) are the dorsal (asterisk) and ventral (double asterisks) surfaces. The type-A trichoid sensilla are found in greatest abundance in a band along the distal (d with arrow) and proximal (p with arrow) margins of the leading, dorsal, and ventral surfaces of each annulus. arrowhead, styliform sensillum complex. **B:** SEM of three adult male antennal flagellar annuli. Leading surface (L) view showing the long, male-specific trichoid sensilla arranged as phalanxes, one pair on the distal (d with arrow) and proximal (p with arrow) margins of the dorsal (asterisk) surface and a similar arrangement of sensilla on the ventral (double asterisks) surface of each annulus. The pairs of phalanxes bend toward each other,

forming an arch (a with line). A band of shorter trichoid sensilla located on the proximal margin of the leading surface connect the phalanxes, forming the scoop (s with line). Arrowhead, styliform sensillum complex. **C:** SEM showing the leading surface of a female flagellar annulus. Type-A trichoid sensilla (arrows) are found in greatest abundance along the distal (arrows) and proximal (arrows with asterisks) margins of the leading (view shown), dorsal, and ventral surfaces of each annulus. Along these margins, these sensilla are found in a band that is 2-3 sensilla deep and are the main sensillum type present. These bands merge toward the trailing surface and form a U-shaped cul-de-sac (not shown), similar but less conspicuous than the pattern of distribution of male-specific trichoid sensilla. **D:** SEM of a higher magnification of the leading surface of female flagellar annulus showing numerous sensillum types. Arrows, type-A coeloconic sensilla; arrows with asterisks, type-B basiconic sensilla; arrowheads, type-A basiconic sensilla; arrowheads with asterisks, type-A trichoid sensilla. Scale bars = 100  $\mu\text{m}$  in A-C, 10  $\mu\text{m}$  in D.



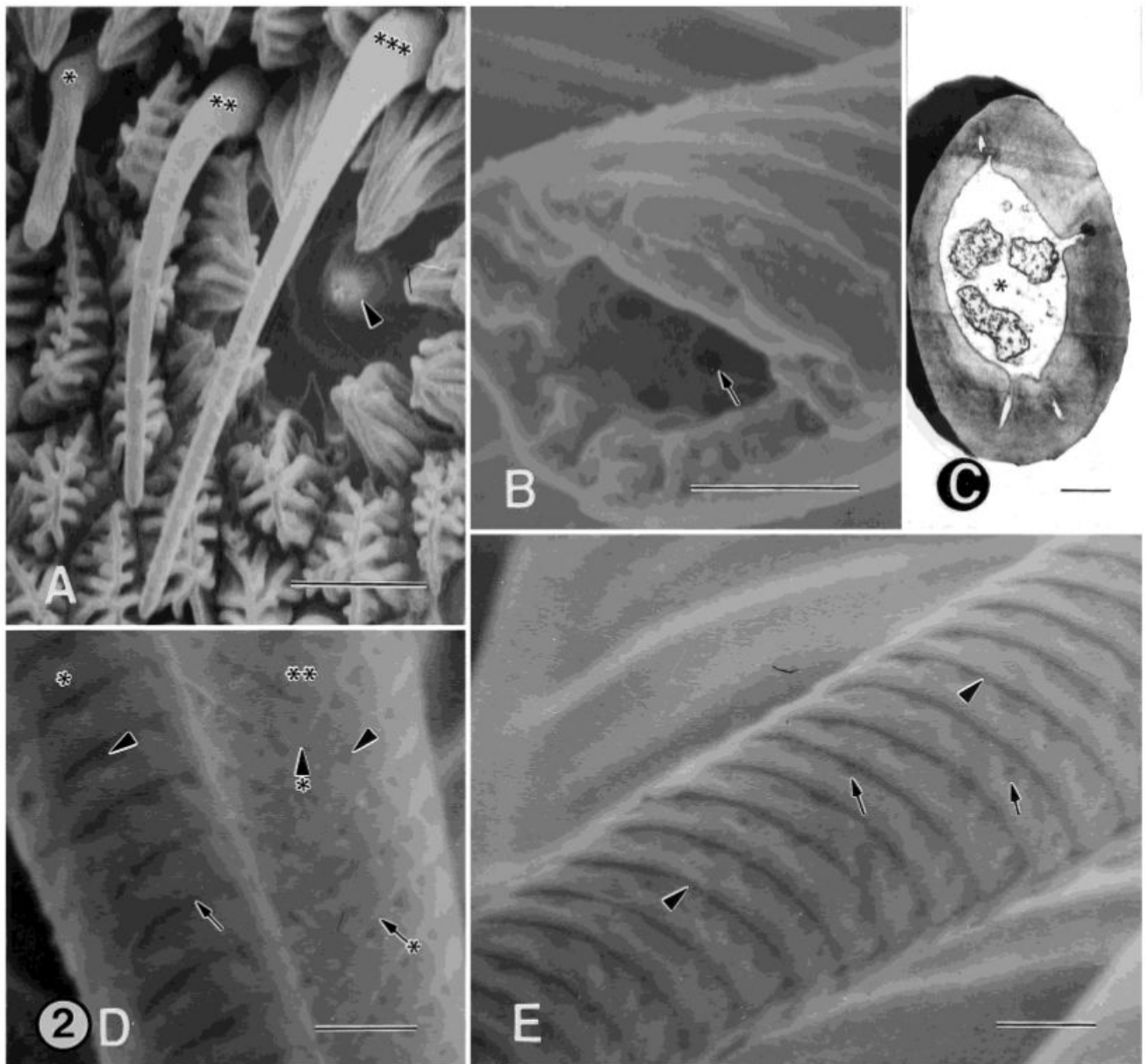


**Fig. 2.**

**A:** SEM of female annulus showing four different sensillum types in close proximity to one another. Asterisk, type-B basiconic sensillum; double asterisks, type-A basiconic sensillum; triple asterisks, type-A trichoid sensillum; arrowhead, type-A coeloconic sensillum. **B:** SEM of the middle portion of the cuticular shaft from a type-A trichoid, single-walled, multiporous sensillum that is broken. This view shows the interior of the cuticular shaft. Three pores (one denoted by the arrow) are visible. The pores extend through the full thickness of the shaft and are visible on the exterior wall of the sensillum, shown in D and E. **C:** TEM of a cross-section of a type-B trichoid sensillum showing three unbranched distal dendrites surrounded by the sensillar sinus (asterisk). **D:** SEM showing the middle portion of the cuticular shafts from a type-A (asterisk) and type-B (double asterisks) trichoid sensillum. The shaft of the type-A sensillum bears circumferential, cuticular ridges (arrow), which form a helical pattern over the basal quarter of its length and a more circular pattern over the remaining length of the sensillum.



The shaft of the type-B sensillum bears diagonal, cuticular ridges (arrow with asterisk), forming a herringbone pattern. The ridges fuse together on one side along the length of the sensillum (arrowhead with asterisk). In both sensillum types, the shafts are perforated by pores (arrowheads). The pores are located in cuticular depressions that extend to the tip of the sensillum and are arranged in a single row along the distal margin of the ridges. **E**: SEM of the middle portion of the cuticular shaft from a type-A trichoid sensillum. Arrowheads, cuticular ridges; arrows, pores. Scale bars = 5  $\mu\text{m}$  in A, 0.5  $\mu\text{m}$  in B-E.

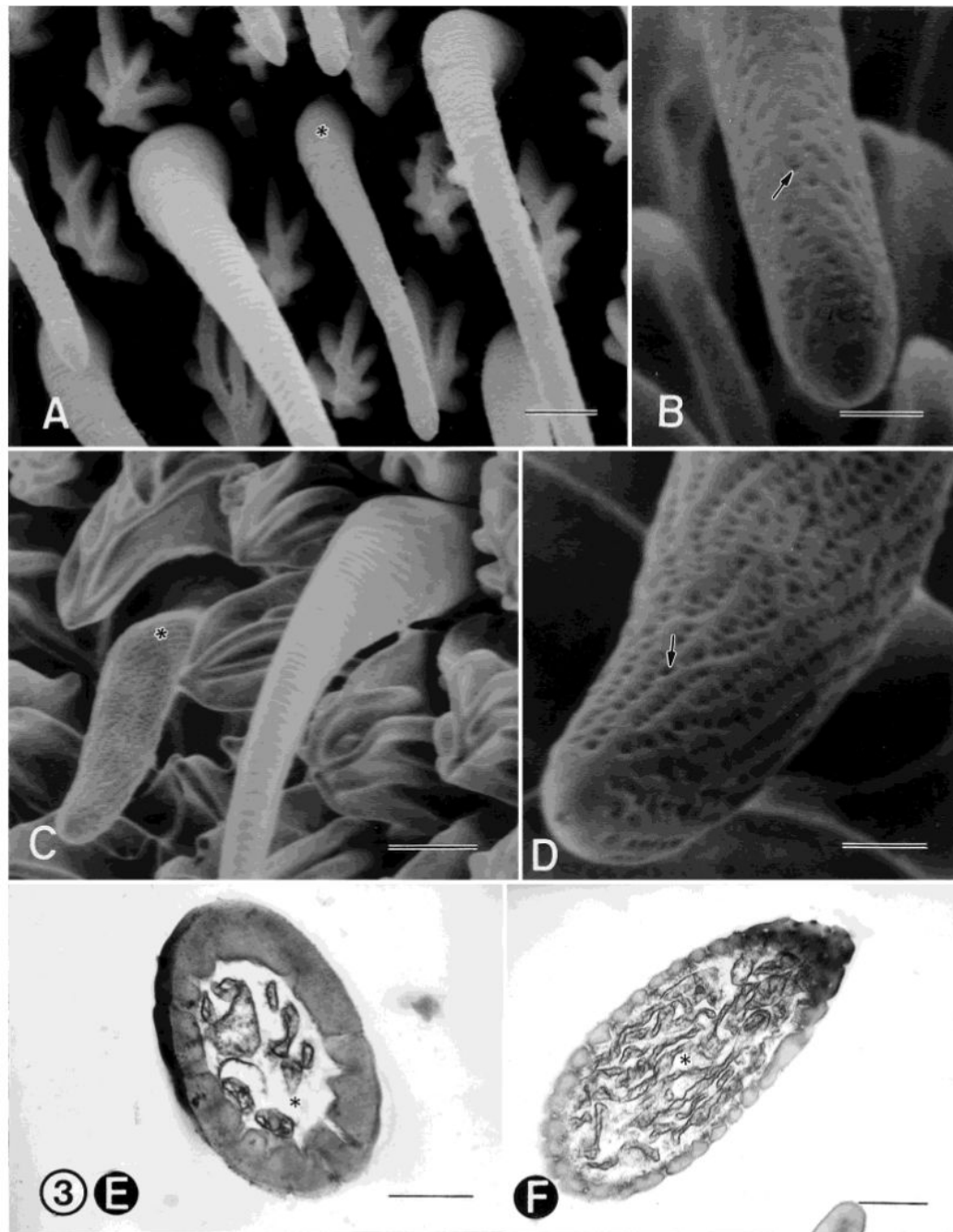


**Fig. 3.**

**A:** SEM showing a type-A basiconic, single-walled, multiporous sensillum (asterisk) between two trichoid type-A sensilla. **B:** SEM of a higher magnification of the cuticular shaft at the distal end of a type-A basiconic sensillum. The pores (arrow) extend to the tip of the sensillum and are distributed in oblique, linear rows along the long axis of the sensillum. **C:** SEM showing a type-B basiconic, single-walled, multiporous sensillum (asterisk) beside a type-A trichoid sensillum. **D:** SEM of a higher magnification of the distal end of the cuticular shaft from the type-B basiconic sensillum shown in C. The pores (arrow) extend to the tip of the sensillum and are distributed in oblique linear rows along the base of deep furrows. The majority of the furrows travel along the long axis of the sensillum, but some travel more obliquely and intersect

adjacent ones. This sensillum type is endowed with many more pores than that of type-A basiconic sensilla. **E:** TEM showing a cross section of a type-A basiconic sensillum with a few distal dendritic branches. Periodic swellings are apparent in some of the branches. Pore tubules do not extend into the shaft lumen. The cuticular wall of this sensillum is about twice as thick as that of a type-B basiconic sensillum. Asterisk, sensillar sinus. **F:** TEM of a cross-section of a type-B basiconic sensillum showing numerous distal dendritic branches. Periodic swellings are apparent in some of the branches. Pore tubules extend into the shaft lumen. Asterisk, sensillar sinus. Scale bars = 2  $\mu\text{m}$  in A,C; 0.5  $\mu\text{m}$  in B,D,E.

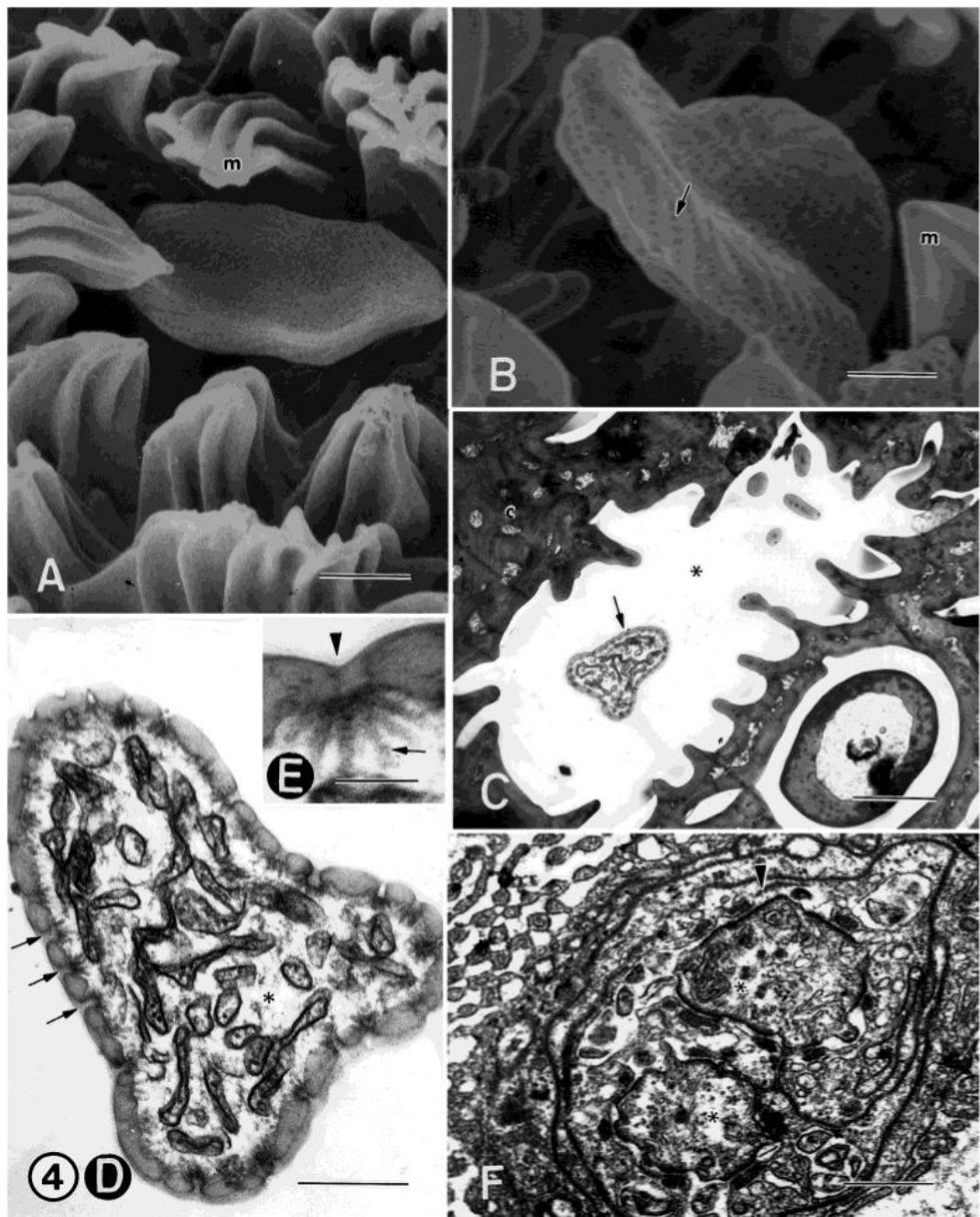


**Fig. 4.**

**A:** FESEM showing an auriculate single-walled, multiporous sensillum. This sensillum resembles an ear or spoon and typically extends only slightly above the level of the microtrichia (m). The upper surface of this sensillum is deeply, concavely indented. **B:** FESEM of another auriculate sensillum endowed with a large number of small pores (arrow), giving the surface cuticle a pitted appearance. m, microtrichia. **C:** TEM showing a low magnification of an auriculate sensillum (arrow) lying in a cuticular pit (asterisk). **D:** TEM of an auriculate sensillum cut near the tip of the sensillum showing numerous distal dendritic branches. The cuticle is very thin and bears numerous pores (arrows). Asterisk, sensillar sinus. **E:** TEM showing a higher magnification of a pore (arrowhead) with underlying pore tubules (arrow).

These pore tubules often appear to contact some of the dendritic branches. **F**: TEM of two proximal dendrites (asterisks) from an auriculate sensillum individually wrapped by the thecogen cell (arrowhead). This cell is in turn wrapped by the trichogen and tormogen cells (not shown). Scale bars = 2  $\mu\text{m}$  in A,C, 1  $\mu\text{m}$  in B, 0.5  $\mu\text{m}$  in D,F, 0.1  $\mu\text{m}$  in E.



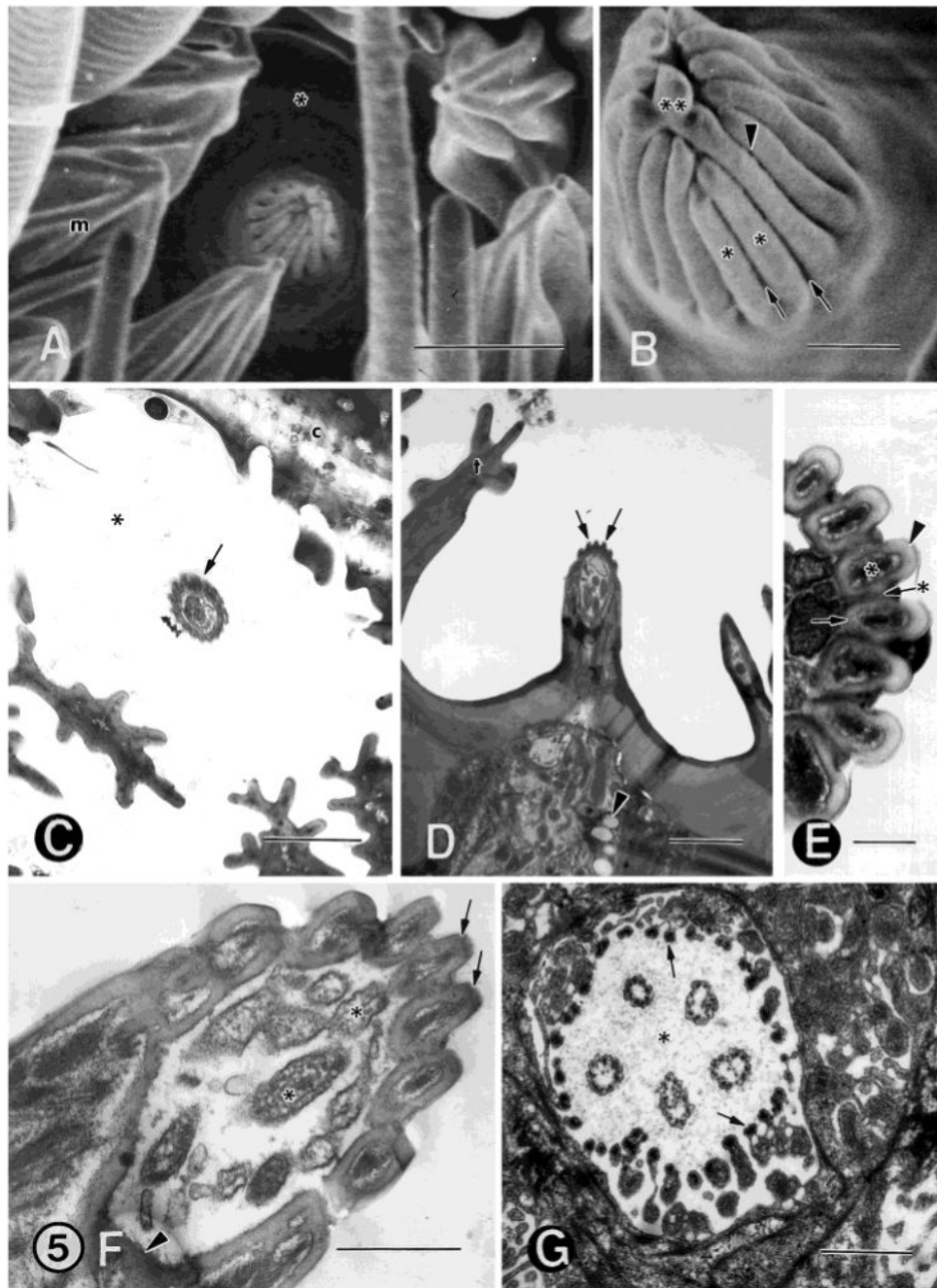


**Fig. 5.**  
**A:** FESEM showing a type-A coeloconic, double-walled, multiporous sensillum. The sensillum lies in a deep pit (asterisk) and is surrounded by microtrichia (m). Seven to ten “teeth” or cuticular spines often form a fringe around the central peg. **B:** FESEM of another sensillum in head-on view at a higher magnification showing 15-16 longitudinal ridges (asterisks). The ridges extend from just above the base to just below the tip of the sensillum. Also shown is a bulbous extension (double asterisks) at the tip of the sensillum, possibly a result of the convergence of two or more ridges. There are grooves (arrows) between the ridges. Very small cuticular pores (arrowhead) are located at the bottom of each groove and are connected with the inside of the sensillum by cuticular spoke channels. **C:** TEM showing a low magnification

of a type-A coeloconic sensillum (arrow) lying in a cuticular pit (asterisk). c, cuticle. **D:** TEM of a longitudinal section showing the conical peg lying in a deep pit. The outer wall is ridged or scalloped (arrows). Globules, presumed to contain lipoidal material (arrowhead), are visible in the sensillar sinus liquor. t, “teeth” or cuticular spines. **E:** TEM showing a higher magnification of seven ridges cut in longitudinal section. There is a double, concentric wall, an inner smooth (arrow) and an outer scalloped or ridged (arrowhead). The cuticular pores are located at the bottom of each groove and connect with the inside of the sensillum by spoke channels (arrow with asterisk), rather than pore tubules. The channels are often filled with a very conspicuous electron-dense material from the sensillar sinus liquor that bathes the distal dendritic branches. The asterisk indicates electron-dense material in lumina between the inner and outer cuticular walls. **F:** TEM longitudinal section of a higher magnification near the tip of the sensillum. The arrows denote the ridged outer wall. The dendritic sheath (arrowhead) begins at the base of the ridges and grooves and encloses the distal dendrites (asterisks). **G:** TEM cross-section cut at the apex of the ciliary dendritic segments showing five distal dendrites enclosed by the thecogen cell (arrows). This cell has become thinner and extends microvilli with discrete complexes of microfibrils, joined at this level by microtubules. These cytoskeletal elements are located along the inner border of this highly infolded cell and adjacent to the ciliary sinus (asterisk). Scale bars = 3  $\mu\text{m}$  in A, 0.5  $\mu\text{m}$  in B,F, 2  $\mu\text{m}$  in C,D, 0.2  $\mu\text{m}$  in E, 1  $\mu\text{m}$  in G.

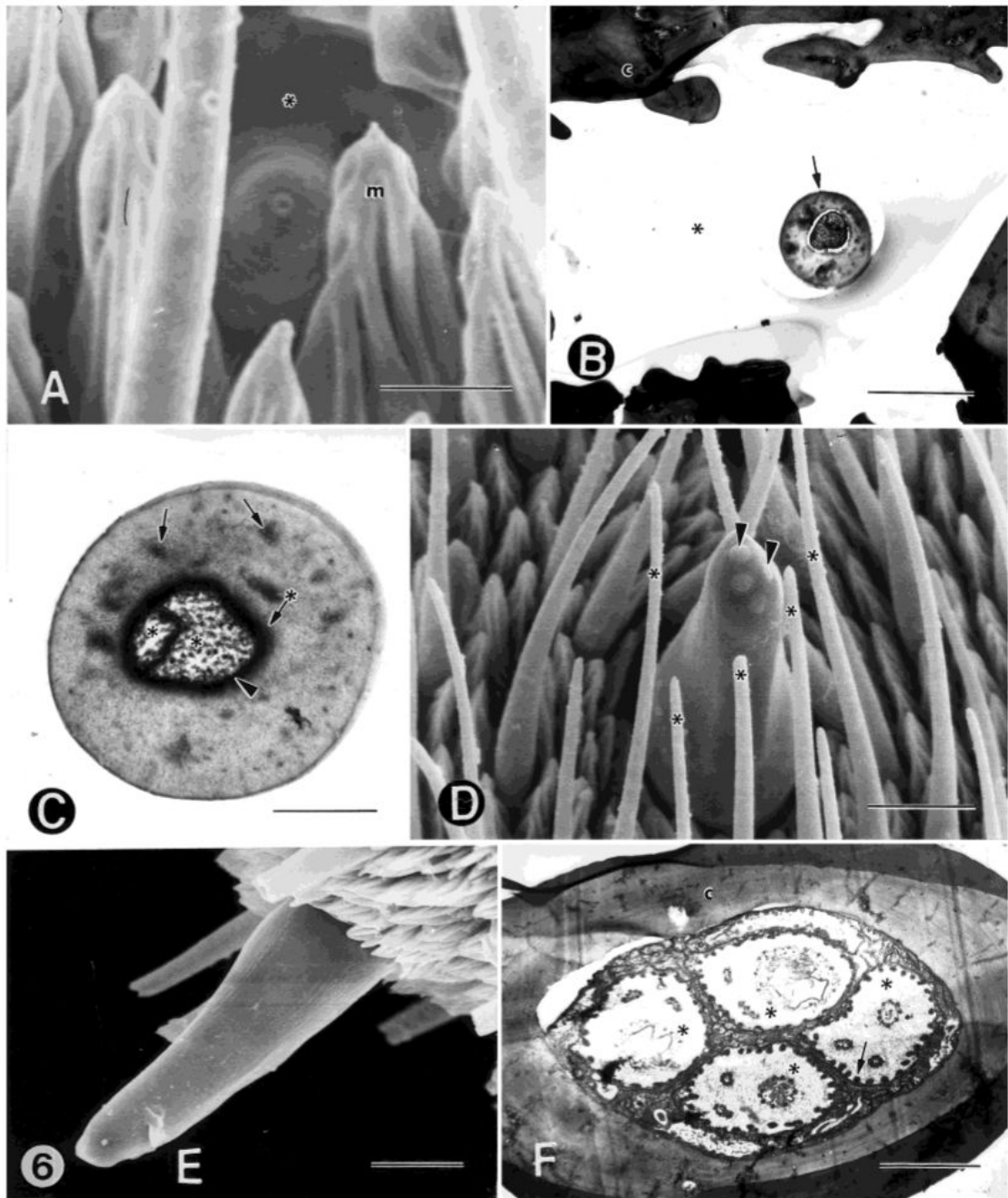


**Fig. 6.**

**A:** FESEM of a type-B coeloconic, single-walled, aporous sensillum. The sensillum lies in a deep pit (asterisk) and is surrounded by microtrichia (m). **B:** TEM of a low magnification of a type-B coeloconic sensillum (arrow) lying in a cuticular pit (asterisk). c, cuticle. **C:** TEM cross-section showing two, voluminous, unbranched distal dendrites (asterisks) that are tightly enclosed by the dendritic sheath (arrowhead), which in turn, is surrounded by a thicker, more electron-dense layer (arrow with asterisk). The distal dendrites fill the sensillum lumen. The second dendrite also terminates near the tip of the sensillum. The sensillum cuticle is thick and contains numerous longitudinal channels (arrows) that end in the wall near the tip of the sensillum. Longitudinal pore tubules fill these channels and extend to the surface of the cuticle

along pore canals. **D:** SEM of a single-walled, aporous styliform complex sensillum. This sensillum has the appearance of a peg and is positioned on the leading surface near the distal margin of each annulus. It occurs singly, is the largest type of sensillum on the antenna, and is mainly surrounded by type-A trichoid sensilla (asterisks). This peg houses several, similar, contiguous sensilla, the number varying according to the location along the flagellum. The arrowheads denote two of several papillae found at the tip of this sensillum. The number of papillae indicate the number of sensilla that are housed within the peg. **E:** SEM of a side view of a styliform complex sensillum. **F:** TEM cross section near the apex of the ciliary sinus, showing four similar, contiguous sensilla (units) (asterisks) housed in this peg. Each unit of the styliform complex sensillum is innervated by three sensory cells: two with large and cylindrical distal dendrites and one with a lamellate distal dendrite and is surrounded by a microvillated thecogen cell (arrow). c, cuticle. Scale bars = 3  $\mu\text{m}$  in A, 2  $\mu\text{m}$  in B,F, 0.5  $\mu\text{m}$  in C, and 10  $\mu\text{m}$  in D,E.

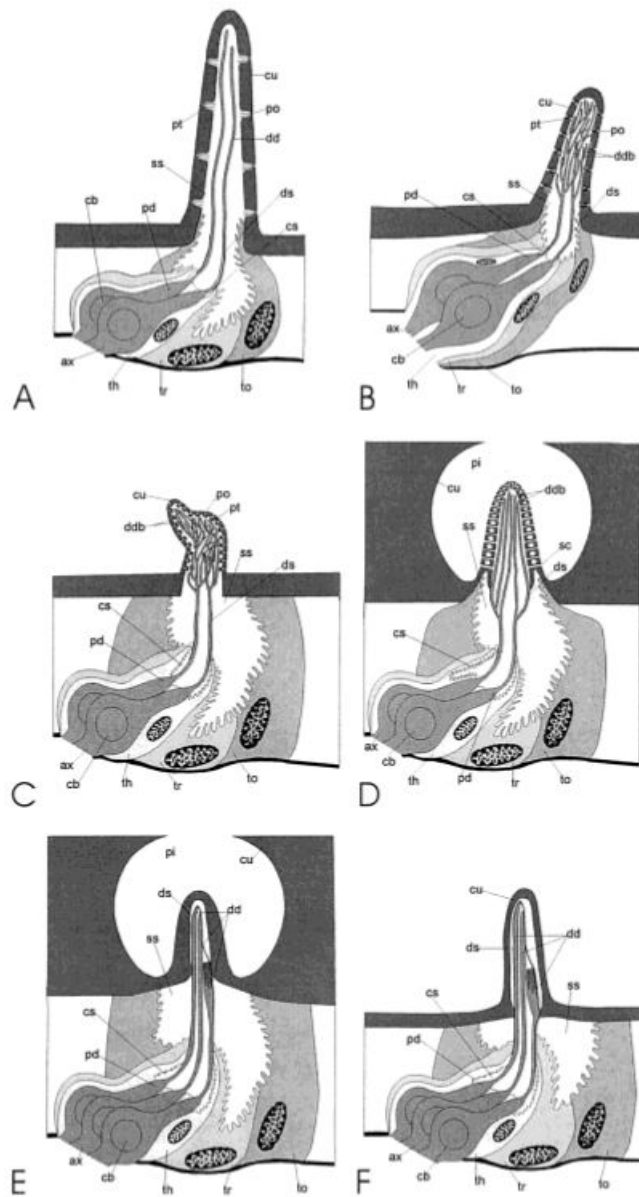


**Fig. 7.** Diagrammatic reconstructions. **A:** Type-A trichoid sensillum; **B:** type-B basiconic sensillum; **C:** auriculate sensillum; **D:** type-A coeloconic sensillum; **E:** type-B coeloconic sensillum; **F:** one of several, similar, contiguous sensilla comprising the styliform complex sensillum on the antennal flagellum of female *M. sexta*. Only two of the three sensory cells are shown for the type-B basiconic sensillum and only two of the five sensory cells are shown for the type-A coeloconic sensillum. The fine structure of the type-B trichoid sensillum and type-A basiconic sensillum is similar that of the type-A trichoid sensillum and type-B basiconic sensillum, respectively, and a diagrammatic reconstruction is not provided for these sensilla. ax, axon; cb, cell body; cs, ciliary sinus; cu, cuticle; ds, dendritic sheath; dd, distal dendrite; ddb, distal dendritic branches; po, pore; pi, pit; pt, pore tubule; pd, proximal dendrite; sc, spoke channel; ss, sensillar sinus; th, thecogen cell; to, tormogen cell; tr, trichogen cell. Reproduced from Shields and Hildebrand, 1999a,b, with permission of the publisher.



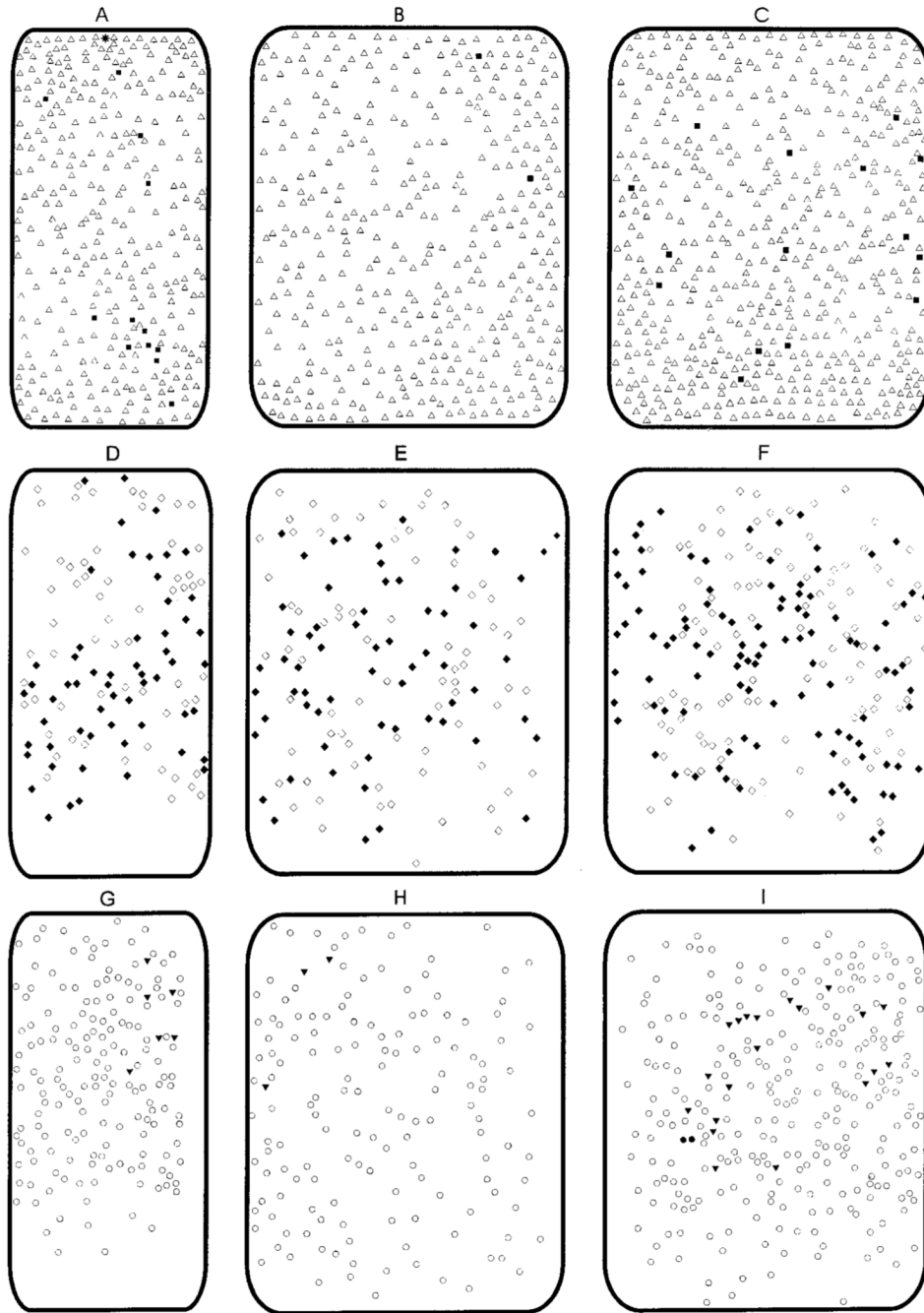


**Fig. 8.** Diagrammatic reconstructions of the leading (**A,D,G**), ventral (**B,E,H**), and dorsal (**C,F,I**) surfaces from a representative antennal flagellar segment (annulus 21, from the base of the flagellum) of female *M. sexta* showing the position of the styliform complex sensillum (filled star), type-A trichoid sensilla (open triangles), type-B trichoid sensilla (filled diamonds), type-A basiconic sensilla (open circles), type-B basiconic sensilla (open diamonds), auriculate sensilla (filled rectangles), type-A coeloconic sensilla (filled triangles), and type-B coeloconic sensilla (filled circles). The trailing surface in each of B and C, E and F, and H and I are to the left and right, respectively. Reproduced from Shields and Hildebrand, 1999b, with permission of the publisher.



weak excitation (<34% of the maximum response); open circles, no response; —, inhibition; no symbol, stimulus not tested. In the case of ORCs 11-13, the responses of individual ORCs in each of four sensilla could not be distinguished unambiguously; therefore the responses from the sensillum were considered to represent those of a single ORC. Each of the pairs of ORCs 6 and 34, 8 and 33, 9 and 30, and 10 and 31 was associated with a single sensillum. Modified from Shields and Hildebrand (2001).

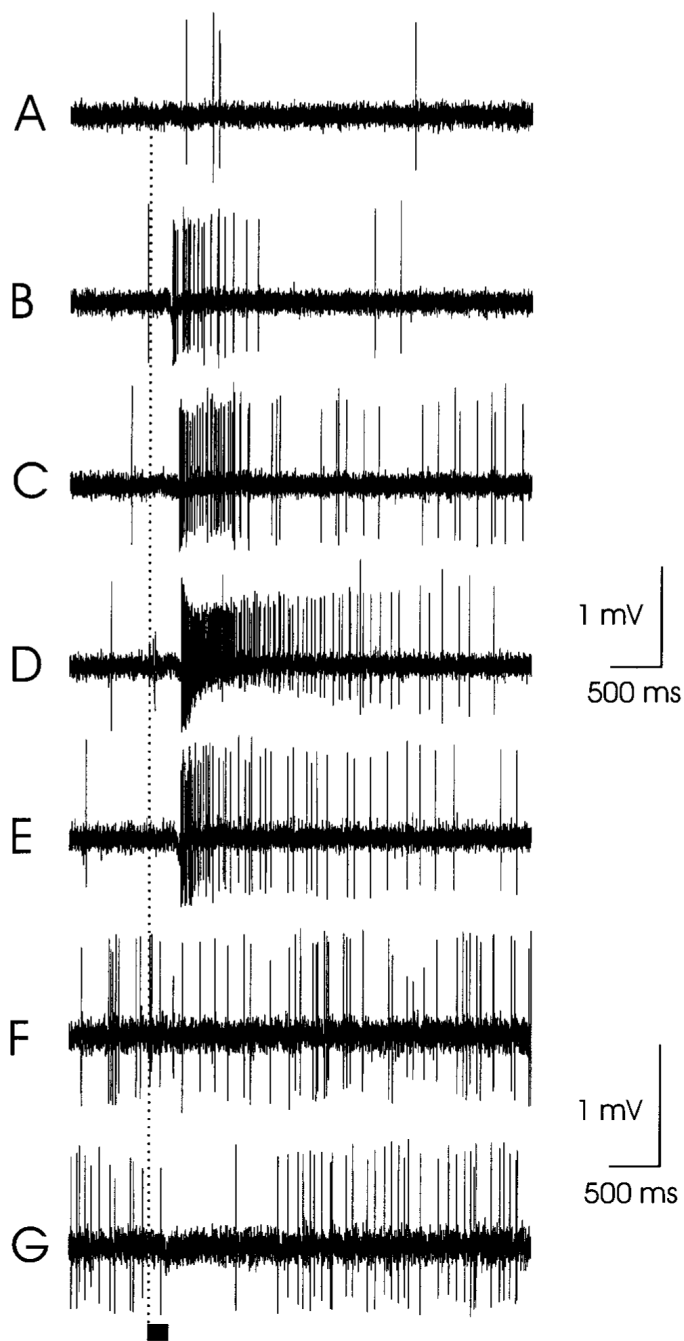


**Fig. 10.** Electrophysiological recordings from two different type-A trichoid sensilla showing excitatory (B-E) and inhibitory (G) responses. Responses of one olfactory receptor cell (ORC) in a sensillum to: **A:** mineral oil alone (blank); **B:** 3  $\mu$ l linalool; **C:** 3  $\mu$ l geraniol; **D:** 3  $\mu$ l *trans*-nerolidol. **E:** Responses of two ORCs in the same sensillum as A-D, above, to headspace volatiles from a *Datura* flower. **F,G:** Responses of one ORC in a different sensillum to (F) mineral oil blank, (G) 3  $\mu$ l 3-octanol. Stimulation with the gaseous phase from olfactometer syringes containing filter paper charged with 30  $\mu$ l of mineral oil solution containing the odorants. Stimulus bar = 200 ms.

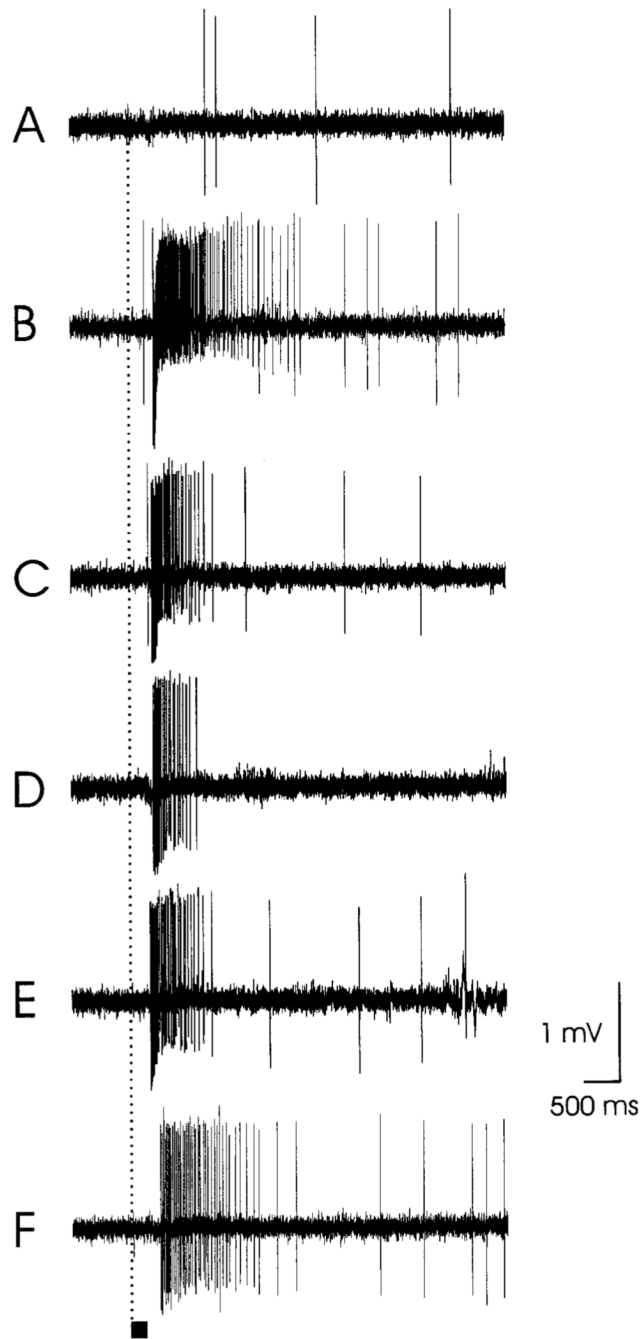


**Fig. 11.** Electrophysiological recordings from a type-A trichoid sensillum showing excitatory (B-F) responses. Responses of one olfactory receptor cell in a sensillum to (A) mineral oil alone (blank); (B) 3  $\mu$ l *cis*-3-hexenylbenzoate; (C) 3  $\mu$ l 2-methylpropylbenzoate; (D) 3  $\mu$ l ethyl-2-aminobenzoate; (E) 3  $\mu$ l ethylsalicylate; (F) 3  $\mu$ l isoamylsalicylate. Stimulation was as described in Figure 10. Stimulus bar = 200 ms.



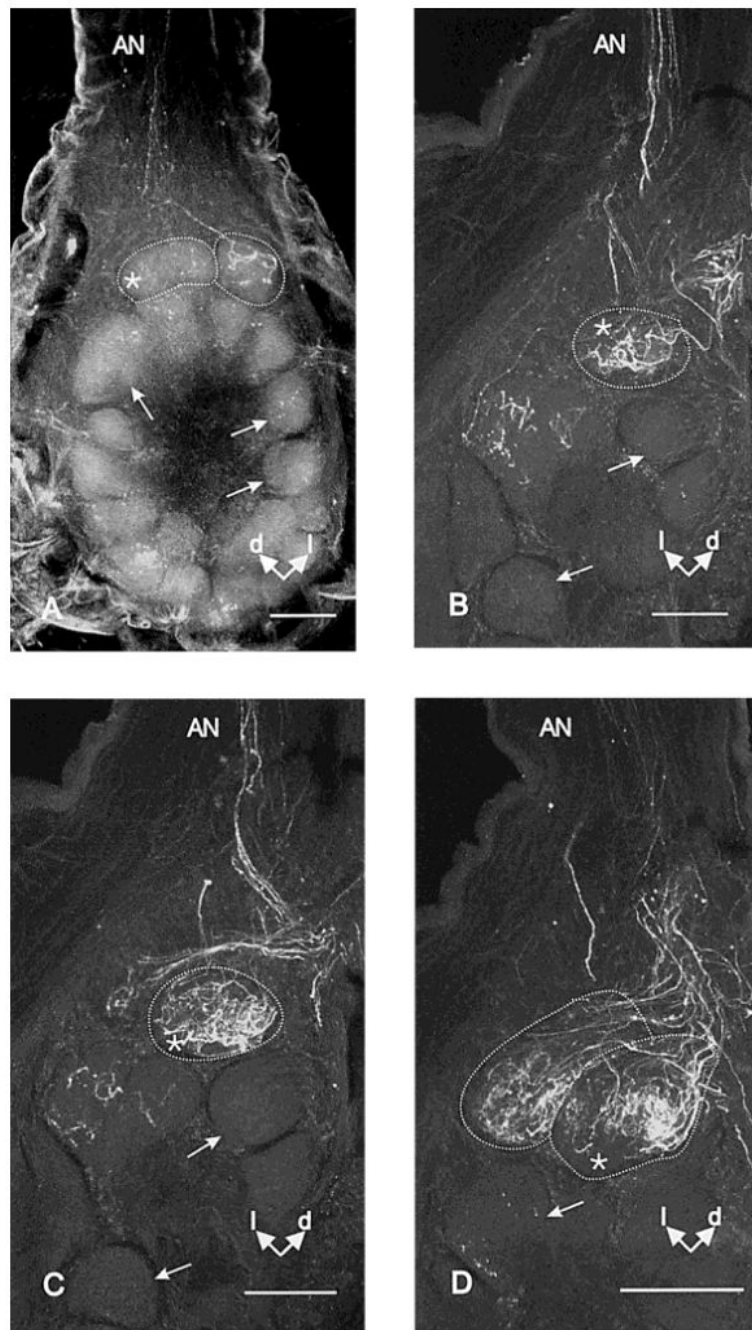


**Fig. 12.** Confocal microscopic images showing central projections of axons from ORCs stained with dextrantetramethylrhodamine. One (B,C) or both (A,D) glomeruli are outlined by a dotted line and represent the sexually dimorphic large female glomeruli (LFGs). The asterisks indicate the median LFG in the dorsolateral region of the antennal lobe, near the site of entry of the antennal nerve (AN). Arrows indicate ordinary, sexually isomorphic glomeruli. d; dorsal; l, lateral. A: Projected serial optical sections of a whole mount showing ORC axons projecting to and terminating in the lateral LFG. B-D: Projected serial optical sections at different depths through the antennal lobe from another specimen. Note ORC axons projecting to and

terminating in both LFGs in D. This specimen is embedded in plastic and sectioned to improve resolution. Scale bars = 100  $\mu\text{m}$

**TABLE 1**  
Types of sensilla on the ventral, dorsal, and leading surfaces on the antennal flagellum of female *Manduca sexta*

Sensillum name	Sensillum type	Sensillum shape	Sensillum length ( $\mu\text{m}$ )	Number and shape of sensory cells	Number of sheath cells	Wall type	Possible function
Type-A trichoid	Multiporous	Hair	34	2; unbranched	3	Single-walled	Olfactory
Type-B trichoid	Multiporous	Hair	26	1, 3; unbranched	3	Single-walled	Olfactory
Type-A basiconic	Multiporous	Peg	22	3; branched	3	Single-walled	Olfactory
Type-B basiconic	Multiporous	Peg	15	3; branched	3	Single-walled	Olfactory
Auriculate	Multiporous	Ear/Spoon	4-5	2; branched	3	Single-walled	Olfactory
Type-A coeloconic	Multiporous	Peg in pit	3.8	5; branched	3	Double-walled	Olfactory/olfactory-thermosensory
Type-B coeloconic	Aporous	Peg in pit	*	3; two unbranched, one lamellate	3	Single-walled	Thermo-hygro-sensory
Styliform complex	Aporous	Peg	38-40	3 per individual sensillum (two unbranched, one lamellate)	3 per individual sensillum	Single-walled	Thermo-hygro-sensory

Modified from Shields and Hildebrand (1999a,b) with permission from NRC Research Press.

\* Not measured.

TABLE 2

Types and numbers of sensilla on the ventral, dorsal, and leading surfaces on female and male flagellar annulus 21 of *Manduca sexta*

Sensillum type on ventral surface	Number of sensilla		Number of sensory cells per annulus	
Type-A trichoid	<b>333</b>	390	<b>666</b>	780
Type-B trichoid	<b>59</b>	315	<b>59-177</b>	822
Type-A basiconic	<b>122</b>	147	<b>366</b>	329
Type-B basiconic	<b>65</b>	68	<b>195</b>	160
Auriculate	<b>21</b>	—	<b>42</b>	—
Type-A coeloconic	<b>8</b>	11	<b>40</b>	55
Total	<b>608</b>	931	1368-1486	2146
<u>Sensillum type on dorsal surface</u>				
Type-A trichoid	<b>469</b>	390	<b>938</b>	780
Type-B trichoid	<b>123</b>	315	<b>123-369</b>	822
Type-A basiconic	<b>250</b>	147	<b>750</b>	329
Type-B basiconic	<b>124</b>	68	<b>372</b>	160
Auriculate	<b>13</b>	—	<b>26</b>	—
Type-A coeloconic	<b>25</b>	11	<b>125</b>	55
Type-B coeloconic	<b>2</b>	—	<b>6</b>	—
Total	<b>1006</b>	931	<b>2340-2586</b>	2146
<u>Sensillum type on leading surface</u>				
Type-A trichoid	<b>287</b>	54	<b>574</b>	108
Type-B trichoid	<b>64</b>	106	<b>64-192</b>	277
Type-A basiconic	<b>152</b>	78	<b>456</b>	175
Type-B basiconic	<b>52</b>	30	<b>156</b>	70
Auriculate	<b>31</b>	—	<b>62</b>	—
Type-A coeloconic	12	—	60	—
Type-B coeloconic	—	3	—	18
Styliform complex	<b>4</b>	6	<b>12</b>	15
Total	<b>602</b>	277	<b>1384-1512</b>	663

Bold typed data from female antennae.

Regular typed data from comparable sensilla of male antennae (Lee and Strausfeld, 1990).

Modified from Shields and Hildebrand (1999b) with permission from NRC Research Press.

— indicates not present.

**TABLE 3**Types and numbers of sensilla on female and male flagellar annulus 21 of *Manduca sexta*

Sensillum types	Number of sensilla		Total number of sensory cells	
Type-A trichoid	<b>1089</b>	834	<b>2178</b>	1664
Type-B trichoid	<b>246</b>	736	<b>246-738</b>	1921
Type-A basiconic	<b>524</b>	372	<b>1572</b>	833
Type-B basiconic	<b>241</b>	166	<b>723</b>	390
Auriculate	<b>65</b>	—	<b>130</b>	—
Type-A coeloconic	<b>45</b>	22	<b>225</b>	110
Type-B coeloconic	<b>2</b>	3	<b>6</b>	9
Styliform complex	<b>4</b>	6	<b>12</b>	18
Total per annulus	<b>2216</b>	2139	<b>5092-5584</b>	4945

Bold typed data from female antennae.

Regular typed data from comparable sensilla of male antennae (Lee and Strausfeld, 1990).

Modified from Shields and Hildebrand (1999b) with permission from NRC Research Press.

— indicates not present.